1521-009X/44/6/842–856$25.00
Drug Metabolism and Disposition
http://dx.doi.org/10.1124/dmd.115.068270
Drug Metab Dispos 44:842–856, June 2016


# RNA Sequencing Quantification of Xenobiotic-Processing Genes in Various Sections of the Intestine in Comparison to the Liver of Male Mice[S]

Zidong Donna Fu, Felcy Pavithra Selwyn, Julia Yue Cui, and Curtis D. Klaassen

*Department of Environmental and Occupational Health Sciences, University of Washington, Seattle, Washington*

Received November 10, 2015; accepted April 4, 2016

## ABSTRACT

**Previous reports on tissue distribution of xenobiotic-processing genes (XPGs) have limitations, because many non–cytochrome P450 phase I enzymes have not been investigated, and one cannot compare the real mRNA abundance of multiple XPGs using conventional quantification methods. Therefore, this study aimed to quantify and compare the mRNA abundance of all major XPGs in the liver and intestine using RNA sequencing. The mRNA profiles of 304 XPGs, including phase I, phase II enzymes, phase II cosubstrate synthetic enzymes, xenobiotic transporters, as well as xenobiotic-related transcription factors, were systematically examined in the liver and various sections of the intestine in adult male C57BL/6J mice. By two-way hierarchical clustering, over 80% of the XPGs had tissue-divergent expression, which partitioned into liver-predominant, small intestine–predominant, and large intestine–predominant patterns. Among the genes, 54% were expressed highest in the liver, 21% in the duodenum, 4% in the jejunum, 6% in the ileum, and 15% in the large intestine. The highest-expressed XPG in the liver was Mgst1; in the duodenum, Cyp3a11; in the jejunum and ileum, Ces2e; and in the large intestine, Cyp2c55. Interestingly, XPGs in the same family usually exhibited highly different tissue distribution patterns, and many XPGs were almost exclusively expressed in one tissue and minimally expressed in others. In conclusion, the present study is among the first and the most comprehensive investigations of the real mRNA abundance and tissue-divergent expression of all major XPGs in mouse liver and intestine, which aids in understanding the tissue-specific biotransformation and toxicity of drugs and other xenobiotics.**

## Introduction

The liver and intestine are two major organs for the absorption, distribution, metabolism, and excretion of xenobiotics. The metabolic reactions of hydrolysis, reduction, and oxidation, catalyzed by phase I enzymes, usually introduce a small functional group to xenobiotic substrates or convert an existing function group to a new group. Xenobiotics and/or their metabolites may be further metabolized via conjugation with a cosubstrate (glucuronide, sulfate, glutathione, amino acids, and methyl or acetyl group) by phase II enzymes. With some exceptions, phase II conjugation reactions are generally considered as major inactivation and detoxification pathways for xenobiotics (Parkinson et al., 2013). The uptake and efflux of xenobiotics and their metabolites, catalyzed by solute carriers (Slc) and ATP-binding cassette (Abc) transporters, respectively, are important for the absorption, distribution, and elimination of xenobiotics (Klaassen and Lu, 2008; Klaassen and Aleksunes, 2010). Many xenobiotic-metabolizing enzymes and transporters are regulated by transcription factors (TFs) (Klaassen and Slitt, 2005; Klaassen and Aleksunes, 2010). In the present study, phase I enzymes, phase II enzymes, enzymes involved in the synthesis of phase II cosubstrates, xenobiotic transporters, and xenobiotic-related TFs are referred to as xenobiotic-processing genes (XPGs). In addition to xenobiotics, many of these XPGs also play a role in the metabolism of endobiotics, such as steroid hormones, fatty acids, bilirubin, and bile acids. It is essential to understand the tissue-specific expression patterns of XPGs, because it facilitates the estimation of the biotransformation and toxicity of various endo- and xenobiotics in those tissues.

Previously, we and others have characterized the expression profiles of many XPGs in the liver and intestine of rodents, including carboxylesterases (Cess) (Jones et al., 2013), aldo-keto reductases (Akrs) (Pratt-Hyatt et al., 2013), cytochrome P450s (P450s) (Renaud et al., 2011), alcohol dehydrogenases (Adhs) (Alnouti and Klaassen, 2008), flavin monooxygenases (Fmos) (Janmohamed et al., 2004),

This work was supported by the National Institutes of Health National Institute of Environmental Health Sciences [Grants ES025708 and ES019487], National Institute of General Medical Sciences [Grant GM111381], and the University of Washington Center for Ecogenetics and Environmental Health [P30 ES007033].
dx.doi.org/10.1124/dmd.115.068270.
[S]This article has supplemental material available at dmd.aspetjournals.org.

**ABBREVIATIONS:** Abc, ATP-binding cassette; Adh, alcohol dehydrogenase; AhR, aryl hydrocarbon receptor; Akr, aldo-keto reductase; Aldh, aldehyde dehydrogenase; ANOVA, analysis of variance; Aox, aldehyde oxidase; Bcrp, breast cancer resistance protein; Bsep, bile salt export pump; CAR, constitutive androstane receptor; Cbr, carbonyl reductase; Ces, carboxylesterase; Ephx, epoxide hydrolase; Fmo, flavin monooxygenase; FPKM, fragments per kilobase of exon per million reads mapped; FXR, farnesoid X receptor; Gst, glutathione-*S*-transferase; HNF, hepatocyte nuclear factor; KUMC, University of Kansas Medical Center; Mat, methionine adenosyltransferase; Mate, multidrug and toxic extrusion protein; Mgst, microsomal Gst; Nat, *N*-acetyl transferase; Nqo, NAD(P)H:quinone oxidoreductase; Nrf2, nuclear factor erythroid 2-related factor 2; Ost, organic solute transporter; Papss, 3′-phosphoadenosine 5′-phosphosulfate synthase; Pept, peptide transporter; P450, cytochrome P450; Pon, paraoxonase; PPAR, peroxisome proliferator-activated receptor; PXR, pregnane X receptor; RNA-Seq, RNA sequencing; RXR, retinoid X receptor; Slc, solute carrier; Slco, solute carrier organic anion; Sult, sulfotransferase; TF, transcription factor; Ugt, UDP-glucuronosyltransferase; XPG, xenobiotic-processing gene.

UDP-glucuronosyltransferases (Ugts) (Shelby et al., 2003; Buckley and Klaassen, 2007), sulfotransferases (Sults) (Dunn and Klaassen, 1998; Alnouti and Klaassen, 2006), glutathione-*S*-transferases (Gsts) (Knight et al., 2007), methyltransferases, *N*-acetyltransferases (Nats), and enzymes for the synthesis of phase II cosubstrates (Lu et al., 2013), as well as various Slc transporters (Li et al., 2002; Slitt et al., 2002; Lu et al., 2004; Ballatori et al., 2005; Cheng et al., 2005; Alnouti et al., 2006; Lu and Klaassen, 2006; Lickteig et al., 2008) and Abc transporters (Brady et al., 2002; Cherrington et al., 2002; Yu et al., 2002; Chen and Klaassen, 2004; Maher et al., 2005, 2006; Tanaka et al., 2005; Cheng and Klaassen, 2009; Cui et al., 2009). Together, these studies have markedly improved our understanding of the tissue-divergent expression patterns of these XPGs.

However, the previous studies have several limitations on the tissue distribution of XPGs. First, the tissue distribution of many non-P450 phase I enzymes, which also play important roles in xenobiotic metabolism, has not been investigated systematically. Second, each of the previous studies focuses on a specific family of XPGs, and there lacks a quantitative comparison of XPGs in all categories in various tissues. Third, most of these studies quantify mRNA of XPGs by conventional mRNA profiling techniques, including northern blot, reverse-transcription–quantitative real-time polymerase chain reaction, microarray, branched DNA, and branched DNA–based multiplex suspension assays. These methods rely on the specificity and efficiency of primer/probe hybridization. With the implementation of RNA sequencing (RNA-Seq) technologies, it is possible to directly compare sequence reads of the nucleotide molecules in biologic samples in a quantitative mode, and thus provide true quantification of the mRNAs of genes. The result of RNA-Seq is expressed as fragments per kilobase of exon per million reads mapped (FPKM), which normalizes the sequencing depths between different samples and sizes between various genes, allowing a direct comparison of various transcripts on a genome-wide scale (Malone and Oliver, 2011). We have previously conducted RNA-Seq experiments on the ontogeny of various XPGs in mouse livers (Cui et al., 2012; Peng et al., 2012, 2013; Lu et al., 2013; Selwyn et al., 2015), but a systematic characterization of the XPGs in various sections of the intestine in comparison with liver tissue is lacking.

Therefore, the goal of the present study was to use RNA-Seq to systematically quantify the mRNA profiles of 304 XPGs in various sections of the intestine [namely, the small intestine (duodenum, jejunum, and ileum) and the large intestine], and compare the intestinal expression of the XPGs with that in livers of male mice. This study also compares the mRNA abundance of various genes within the same gene family/category and across different families/categories in these tissues. This knowledge will shed light on the tissue-specific differences in the pharmaco- and toxicokinetic profiles of xenobiotics.

## Materials and Methods

**Animals.** All mice used in the studies were male C57BL/6J mice (2–3 months of age, $n = 3$) purchased from Jackson Laboratory (Bar Harbor, ME), and were housed in an Association for Assessment and Accreditation of Laboratory Animal Care International–accredited facility at the University of Kansas Medical Center (Kansas City, KS), with a 14-hour light/10-hour dark cycle, in a temperature and humidity-controlled environment. All mice were given ad libitum access to the standard autoclaved rodent chow #5K67 (LabDiet, St. Louis, MO) and autoclaved water. All animal experiments were approved by the Institutional Animal Care and Use Committee at the University of Kansas Medical Center (KUMC).

**Tissue Collection.** Tissues were harvested from mice between 9 a.m. and noon to minimize the diurnal variations in XPG expression (Zhang et al., 2009). Animals were not fasted before tissue collection because food restriction is known to alter XPG expression in the liver (Fu and Klaassen, 2014). Livers were collected after removing the gallbladder. Intestinal contents were flushed with phosphate-buffered saline, and intestinal tissues were separated into various sections [namely, duodenum, jejunum, ileum, and large intestine (colon)]. All tissues were snap-frozen in liquid nitrogen and stored at −80°C.

**Total RNA Isolation.** Total RNA was isolated from tissues using RNA Bee reagent (Tel-Test Inc., Friendswood, TX) following the manufacturer's protocol. The concentration of total RNA in each sample was quantified spectrophotometrically at 260 nm using a NanoDrop 1000 Spectrophotometer (Thermo Scientific, Waltham, MA). RNA integrity was confirmed using a dual Agilent 2100 Bioanalyzer (Agilent Technologies Inc., Santa Clara, CA), and the samples with RNA integrity numbers above 7.0 were used for the following experiments.

**cDNA Library Preparation and RNA-Seq.** The cDNA library preparation and sequencing of the transcriptome were performed in the KUMC Genome Sequencing Facility. The cDNA libraries from total RNA samples ($n = 3$/group) were prepared using an Illumina TruSeq RNA sample prep kit (Illumina, San Diego, CA). Three micrograms of total RNA was used as the RNA input according to the manufacturer's protocol. The mRNAs were selected from the total RNAs by purifying the poly-A–containing molecules using poly-T primers. The RNA fragmentation, first- and second-strand cDNA syntheses, end repair, adaptor ligation, and polymerase chain reaction amplification were performed according to the manufacturer's protocol. The average size of the cDNAs was approximately 160 bp (excluding the adapters). The cDNA libraries were validated for RNA integrity and quantity using an Agilent 2100 Bioanalyzer (Agilent Technologies Inc.) before sequencing. The cDNA libraries were clustered onto a TruSeq paired-end flow cell and sequenced ($2 \times 50$ bp) using a TruSeq SBS kit (Illumina) on an Illumina HiSeq2000 sequencer (KUMC Genome Sequencing Facility) with a multiplexing strategy of four samples per lane.

**RNA-Seq Data Analysis.** After the sequencing platform generated the sequencing images, the pixel-level raw data collection, image analysis, and base calling were performed by Illumina's Real Time Analysis (RTA) software on a Dell PC (Dell, Round Rock, TX) attached to a HiSeq2000 sequencer. The base call files (*.BCL) were converted to qseq files by Illumina's BCL Converter, and the qseq files were subsequently converted to Fastq files for downstream analysis. The RNA-Seq reads from the Fastq files were mapped to the mouse reference genome (UCSC mm10) (https://genome.ucsc.edu), and the splice junctions were identified by TopHat2 (http://tophat.cbcb.umd.edu/). The output files in binary sequence alignment format were analyzed by Cufflinks (http://cufflinks.cbcb.umd.edu/) to estimate the transcript abundance. The mRNA abundance was expressed as the number of FPKM. The data discussed in this publication have been deposited in the National Center for Biotechnology Information's Gene Expression Omnibus and are accessible through Gene Expression Omnibus series accession number GSE79848.

**Statistical Analysis.** Data are presented as the mean FPKM ± S.E.M. XPGs with mean FPKM values smaller than 1 per tissue in all five tissues were defined as not expressed in the liver or intestine. Differences between various groups were determined using a one-way analysis of variance (ANOVA) followed by Duncan's post-hoc test, with significance set at $p < 0.05$. The ANOVA was performed using SPSS 16.0 software (IBM Corporation, Armonk, NY). The FPKM values were $\log_2$-transformed to achieve normal distribution prior to the ANOVA. Any groups with the same letter are not statistically different from each other. To determine the tissue distribution patterns of XPG expression, a two-way hierarchical clustering dendrogram (Ward's minimum variance method, distance scale) was generated by JMP 12.1.0 software (SAS Institute, Inc., Cary, NC) for the mean mRNA expression of differentially expressed XPGs ($p < 0.05$, ANOVA). The expression in various tissues was standardized within a gene to present the tissue-differential expression pattern. High mRNA abundance is presented in red, whereas low mRNA abundance is in blue. Relative color intensities are not comparable between genes.

## Results

### Summary of the mRNA Expression of All XPGs in Liver and Intestine of Adult Male C57BL/6J Mice

RNA-Seq generated approximately 40–80 million reads per sample at each end, with approximately 70–160 million reads mapped to the mouse reference genome (UCSC mm10). The percentage of mapped reads was approximately 95–97%. The total FPKM values of the entire transcriptome were similar among the five adult mouse tissues of the

liver, duodenum, jejunum, ileum, and large intestine. This was consistent with equal loading of total cDNA libraries from these samples on RNA-Seq. In total, 304 XPGs with known important functions in xenobiotic metabolism and transport functions were analyzed. These genes belong to various categories—namely, 156 phase I enzymes, 81 phase II enzymes, 35 uptake transporters, 21 efflux transporters, and 11 TFs (Table 1). The FPKM values of all XPGs in liver and intestine of individual mice are shown in Supplemental Table 1. The cumulative mRNA abundance of all XPGs displayed marked tissue-divergent expression patterns, which was highest in the liver, medium in the duodenum (about 50% of liver), and lowest in the jejunum, ileum, and large intestine (Fig. 1A). A similar tissue-specific pattern was observed for the cumulative mRNA expression of both phase I and phase II enzymes. The cumulative mRNAs of the uptake were highest in both the liver and ileum, and lowest in the large intestine, whereas the cumulative mRNAs of the efflux transporters were highest expressed in the ileum and lowest in the large intestine. In comparison, the cumulative mRNAs of TFs were less divergent among tissues.

As shown in Fig. 1B, among the 304 XPGs, 51 (16.8%) genes were not expressed in the liver or intestine, which was defined as mean FPKM values less than 1 in all five tissues, whereas 252 (82.9%) were differentially expressed in at least two tissues ($p < 0.05$, one-way ANOVA followed by Duncan's post-hoc test), and peptide transporter 2 (Pept2/Slc15a2) was relatively equally expressed among all of the tissues. The XPGs that were not expressed in the liver or intestine are listed in Table 2, which includes 18 phase I enzymes, 19 phase II enzymes, 11 uptake transporters, and 3 efflux transporters.

To determine the tissue-specific expression patterns of the 252 differentially expressed XPGs, a two-way hierarchical clustering dendrogram was generated using their standardized mean FPKM values (Fig. 1C). These XPGs were partitioned into three distinctive expression patterns: liver-predominant (cluster 1), small intestine–predominant (cluster 2), and large intestine–predominant (cluster 3). A larger Fig. 1C is shown in Supplemental Fig. 1, A–C. The cumulative FPKM values of genes in each cluster are plotted in Fig. 1D. The number of XPGs with the highest FPKMs in each tissue is shown in Fig. 1E, which is 136 (54%) in the liver, 53 (21%) in the duodenum, 10 (4%) in the jejunum, 16 (6%) in the ileum, and 37 (15%) in the large intestine. The FPKMs of individual XPGs were further described by gene families.

TABLE 1

List of 304 XPGs with known importance in xenobiotic metabolism and transport functions

| Gene Category (Gene No.) | Gene Family (Gene No.) |
|---|---|
| Phase I enzymes (156) | Cess (18) |
| | Pons (3) |
| | Ephxs (2) |
| | Akrs (16) |
| | Cbrs (4) |
| | Nqos (2) |
| | P450s (76) |
| | Por |
| | Adhs (6) |
| | Aldhs (20) |
| | Aoxs (3) |
| | Fmos (5) |
| Phase II enzymes (81) | Ugts (21) |
| | Sults (17) |
| | Gsts (25) |
| | Methyltransferases (3) |
| | Nats (3) |
| | Amino acid conjugation enzymes (3) |
| | Enzymes that synthesize conjugation cofactors (9) |
| Uptake transporters (35) | Slcs (35) |
| Efflux transporters (21) | Abcs (17) |
| | Mates (2) |
| | Osts (2) |
| TFs (11) | NRs (8) |
| | AhR, HNF1$\alpha$, Nrf2 |

NRs, nuclear receptors; Por, P450 (cytochrome) oxidoreductase.

## Tissue Distribution of Phase I Enzymes in Liver and Intestine of Adult Male C57BL/6J Mice

**Phase I Enzymes Involved in Hydrolysis Reactions.** Cess catalyze the hydrolysis and trans-esterification of various esters and amides, which mainly results in the inactivation of drugs (e.g., heroin, cocaine, and flumazenil), as well as the activation of some prodrugs (e.g., irinotecan) (Redinbo and Potter, 2005). Five subfamilies of Ces genes, for a total of 18 genes, are presented in this study. As shown in Fig. 2A, the cumulative FPKM of all Ces mRNAs was highest in the liver, medium in the small intestine (duodenum > jejunum = ileum), and lowest in the large intestine. The most abundantly expressed Ces mRNAs in the liver were Ces1c and 3a, whereas in the intestine, Ces2a, 2c, and 2e were the most abundantly expressed. Three Ces mRNAs were not expressed in the liver or intestine: Ces1a, 2f, and 5a (Table 2). The Ces genes within the same subfamily tended to have the same tissue distribution pattern. Ces1b and 1c mRNAs were almost exclusively expressed in the liver. Ces1d-1g mRNAs were also highest in the liver and lower in the intestine. The Ces2 subfamily was highest expressed in the duodenum (Ces2a, 2b, 2c, 2e, and 2g), whereas the Ces3 subfamily (Ces3a and 3b) and Ces4a were almost exclusively expressed in the liver.

Paraoxonases (Pons) hydrolyze a broad range of organophosphates, aromatic carboxylic acid esters, cyclic carbonates, and lactones (Parkinson et al., 2013). There are three Pons in the mouse genome, and the cumulative FPKM of all Pons was highest in the liver and about 75% lower in the intestine (large intestine = duodenum > jejunum = ileum) (Fig. 2B). The most abundantly expressed Pon in the liver was Pon1, whereas in both the small and large intestine, Pon2 was the most abundantly expressed. Three Pons had distinctive expression patterns among tissues: Pon1 was almost exclusively expressed in the liver; Pon2 mRNA was highest in the duodenum and large intestine, medium in the jejunum and ileum, and lowest in the liver; and Pon3 mRNA was highest in the liver and large intestine, medium in the duodenum, and lowest in the jejunum and ileum.

Epoxide hydrolases (Ephxs) catalyze the hydrolysis and detoxification of electrophilic epoxides, which otherwise may lead to cellular and genetic toxicity through protein and nucleic acid binding. Mice have two Ephxs that are important in xenobiotic metabolism: the microsomal form Ephx1 and the soluble form Ephx2. As shown in Fig. 2C, the cumulative FPKM of the two Ephxs was highest in the liver, medium in the small intestine (duodenum > jejunum = ileum), and lowest in the large intestine. Ephx1 mRNA was much higher in the liver than in the intestine, whereas Ephx2 mRNA was highest in both the liver and duodenum, medium in the jejunum and ileum, and lowest in the large intestine.

**Phase I Enzymes Involved in Reduction Reactions.** Akrs are cytosolic enzymes that are responsible for the reduction of aldehydes and ketones to primary and secondary alcohols, respectively (Parkinson et al., 2013). In addition to xenobiotic metabolism, some Akrs are also involved in bile acid synthesis as well as the metabolism of steroid hormones and carbohydrates. There are two families of Akrs (16 genes in total) in mice, and Akr1 is the larger family with five subfamilies (Akr1a–e) that include 15 genes. The cumulative FPKM of all Akrs was highest in the liver, medium in the duodenum, and lowest in the jejunum, ileum, and large intestine (Fig. 3A). The most abundantly expressed Akr in the liver was Akr1c6, and in the intestine, Akr1a1/1a4. Akr1c18 and 1c21 were not expressed in the liver or intestine (Table 2). Individual

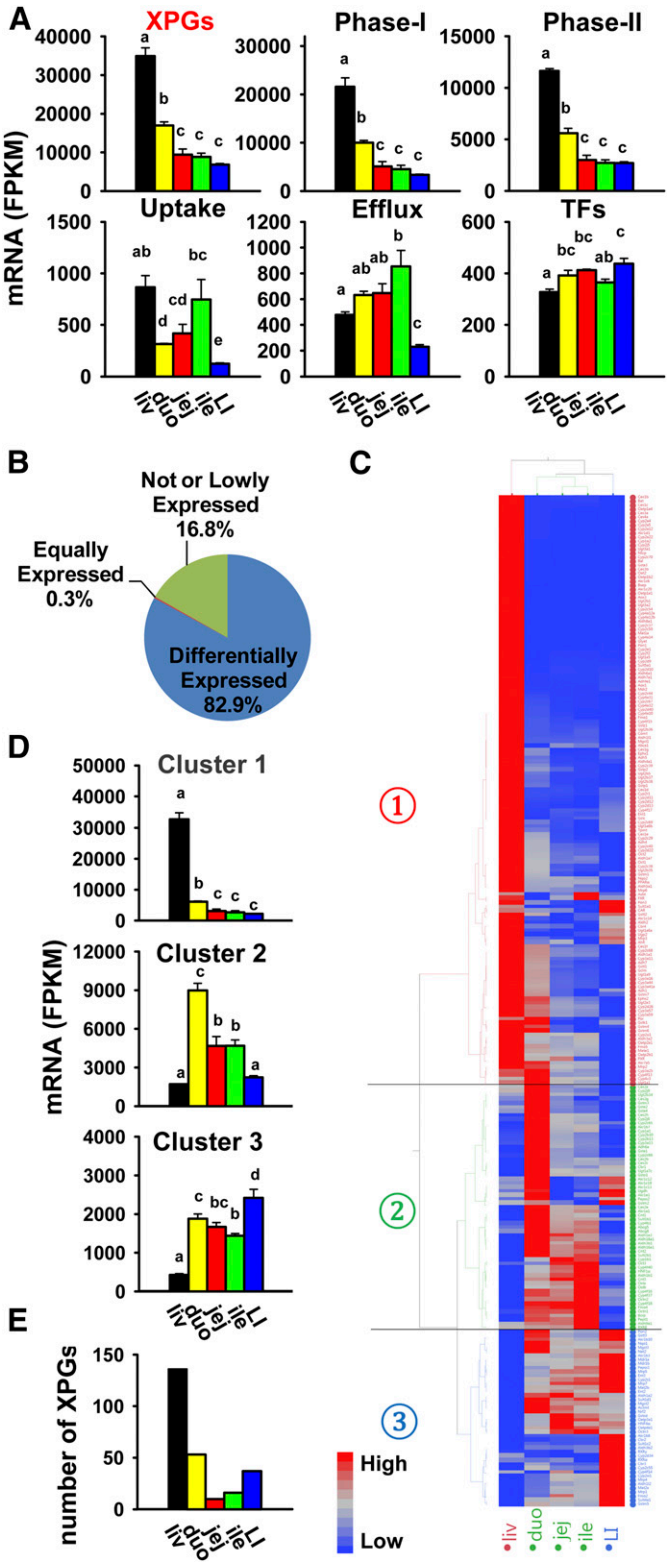


**Fig. 1.** Summary of the mRNA expression of all XPGs in the liver and intestine. Liver (liv) and various sections of the intestine [duodenum (duo), jejunum (jej), ileum (ile), and large intestine (LI)] from C57BL/6J male mice ages 2–3 months were used for RNA-Seq quantification. (A) Tissue distribution of cumulative mRNAs of all XPGs and genes in each category (namely, phase I enzymes, phase II enzymes, uptake transporters, efflux transporters, and transcription factors). Data are presented as the mean FPKM ± S.E.M. of three individual animals. Any groups with the same letter are not different from each other (significance set at $p < 0.05$, one-way ANOVA followed by Duncan's post-hoc test). (B) Percentages of the 304 XPGs that are not expressed, equally expressed, or differentially expressed in the liver and intestine. (C) Two-way hierarchical clustering of the 252 XPGs with differential expression in at least two tissues. The dendrogram describes the relationship between different gene expression profiles and various tissues. Average FPKM values of three mice per tissue are presented by colored squares: red, relatively high expression; blue, relatively low expression. The solid lines separate the expression profiles into three clusters of liver-predominant, small intestine–predominant, and large intestine–predominant expression. (D) Cumulative mRNAs of genes in each cluster in the liver and intestine. (E) Number of XPGs with highest mRNA expression in each tissue.

TABLE 2

List of 51 XPGs that are not expressed in the liver or intestine (mean FPKM <1 in all five tissues)

| Gene Category (Gene No.) | Gene Name |
|---|---|
| Phase I enzymes (18) | Ces1a, 2f, 5a |
| | Akr1c18, 1c21 |
| | Cyp2b9, 2b19, 2b23, 2g1, 2j8, 2j11, 2j13, 2t4, 4f39, 4x1 |
| | Aldh3a1 |
| | Aox3l1 |
| | Fmo3 |
| Phase II enzymes (19) | Ugt1a2, 1a10, 2a1, 2a2, 8a |
| | Sult1c1, 1e1, 2a1, 2a2, 2a3, 2a4, 2a5, 2a7, 3a1, 6b1 |
| | Gsto2, t4 |
| | Nat1, 3 |
| Uptake transporters (11) | Oat1, 3 |
| | Urat1 |
| | Oatp1a5, 1a6, 1c1, 4c1, 5a1, 6b1, 6c1, 6d1 |
| Efflux transporters (3) | Mate2 |
| | Mrp8, 9 |

Akrs had divergent expression patterns among tissues. Some were highest expressed in the liver and much lower in the intestine (Akr1c6, 1c14, 1c20, and 1d1), some were highest expressed in the duodenum (Akr1a1/1a4 and 1b7), some were highest expressed in both the duodenum and large intestine (Akr1b10, 1c12, 1c13, and 1c19), and some were highest expressed in the large intestine (Akr1b3 and 1b8). Akr1e1 had much less divergent expression among tissues. Akr7a5 mRNA was highest in both the liver and duodenum, medium in the jejunum and ileum, and lowest in the large intestine.

Carbonyl reductases (Cbrs), which belong to the large short-chain dehydrogenase/reductase family, play a role in the reduction of a wide variety of carbonyl-containing xenobiotics, such as haloperidol, pentoxifylline, and doxorubicin (Rosemond and Walsh, 2004). There are four Cbrs in the mouse genome, and the cumulative FPKM of all Cbrs was highest in the duodenum; medium in the jejunum, ileum, and large intestine; and lowest in the liver (Fig. 3B). Cbr1 was the most abundantly expressed Cbr in all tissues, and it was highest expressed in the duodenum. Cbr2 and 3 mRNAs were highest in the large intestine and minimal or much lower in the liver and small intestine, whereas Cbr4 mRNA was highest in the liver and lower in both the small and large intestine.

NAD(P)H:quinone oxidoreductases (Nqos) are responsible for the two-electron reduction of quinones to stable hydroquinones, which competes with the one-electron reduction of quinones to semiquinone radicals that lead to cellular and genetic toxicity (Parkinson et al., 2013). Mice have two Nqos, and the cumulative FPKM of these Nqos was highest in the duodenum, followed by the jejunum, ileum, and large intestine at comparable levels, and lowest in the liver (Fig. 3C). Nqo1 mRNA was intestine-enriched (highest in the duodenum, followed by the large intestine, jejunum, and ileum) and markedly lower in the liver. In contrast, Nqo2 mRNA was highest in the liver,

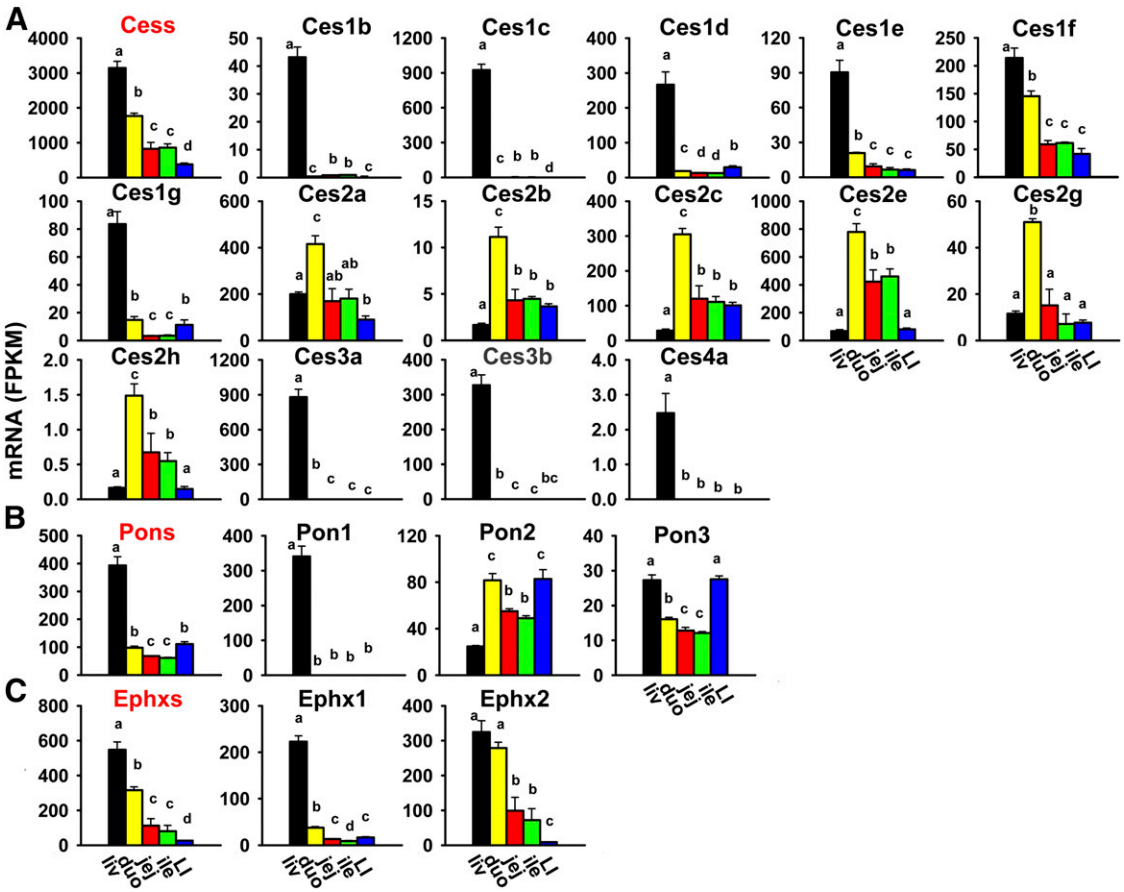


**Fig. 2.** Tissue distribution of Ces (A), Pon (B), and Ephx (C) mRNAs in the liver and intestine. Data are presented as the mean FPKM ± S.E.M. of three individual animals. Any groups with the same letter are not different from each other (significance set at $p < 0.05$, one-way ANOVA followed by Duncan's post-hoc test). The tissue distribution of cumulative mRNAs of genes in each gene family are shown with a red title. duo, duodenum; ile, ileum; jej, jejunum; LI, large intestine; liv, liver.

lower (less than 50% of liver) in the small intestine, and lowest in the large intestine.

### Phase I Enzymes Involved in Oxidation Reactions

P450s are a class of heme-containing monooxygenases that rank among the top most important xenobiotic-metabolizing enzymes in terms of their catalytic versatility and wide spectrum of xenobiotics they detoxify or activate to reactive intermediates (Parkinson et al., 2013). P450s involved in xenobiotic transformation primarily belong to the first three families (Cyp1–3), and substrates for the Cyp4 family mainly include fatty acids and eicosanoids, but also include some xenobiotics. Mice have 102 P450s, and many of the newly identified P450s are still considered "orphans" with no known functions (Nelson et al., 2004). The tissue distribution of 76 P450s in the Cyp1 to Cyp4 families was investigated in mice. As shown in Fig. 4, the cumulative FPKM of these 76 P450s was highest in the liver, medium in the duodenum (less than 50% of liver), and lowest in the jejunum, ileum, and large intestine. The most abundantly expressed P450s in the liver were Cyp2e1 and 3a11; in the duodenum, Cyp3a11 and 2b10; in the jejunum and ileum, Cyp3a11 and 4v3; and in the large intestine, Cyp2c55. Ten P450s were not expressed in the liver or intestine: Cyp2b9, 2b19, 2b23, 2g1, 2j8, 2j11, 2j13, 2t4, 4f39, and 4x1 (Table 2). Most P450s in the Cyp1–4 families were highest expressed in the liver, including Cyp1a2, most Cyp2 (2a4, 2a5, 2a12, 2a22, 2c29, 2c37, 2c38, 2c39, 2c40, 2c44, 2c50, 2c54, 2c67, 2c68, 2c69, 2c70, 2d9, 2d10, 2d11, 2d12, 2d13, 2d22, 2d26, 2d40, 2e1, 2f2, 2j5, 2r1, and 2u1), most Cyp3 (3a11, 3a16, 3a41a, 3a44, 3a57, and 3a59), and some Cyp4 (4a10, 4a12a, 4a12b, 4a14, 4a31, 4a32, 4f15, and 4f17) family members (Figs. 4 and 5A). Others were highest expressed in the duodenum (Cyp1a1, 2b10, 2b13, 2c65, 2c66, 2j6, 2j9, 3a13, 3a25, 4b1, 4f13, and 4v3), jejunum (Cyp1b1, 4f14, and 4f18), ileum (Cyp4f16, 4f37, and 4f40), or large intestine (Cyp2c55, 2d34, 2w1, and 2s1). Noticeably, many were almost exclusively expressed in the liver (Cyp1a2, 2a4, 2a5, 2a12, 2a22, 2c37, 2c44, 2c50, 2c54, 2c67, 2c70, 2d9, 2d10, 2d40, 2e1, 2f2, 2j5, 4a10, 4a12a, 4a12b, 4a14, 4a31, 4a32, and 4f15), and some were almost exclusively expressed in the small intestine (Cyp1a1 and 2c66).

P450 (cytochrome) oxidoreductase transfers electrons from NADPH to P450s to facilitate their catalytic functions. The P450 (cytochrome) oxidoreductase mRNA was moderately higher in the liver and duodenum, and lower in the jejunum, ileum, and large intestine (Fig. 5A).

Adhs, which belong to the medium-chain dehydrogenases/reductases, metabolize a wide range of substrates, including ethanol, retinol, other aliphatic alcohols, hydroxysteroids, and lipid peroxidation products (Duester et al., 1999). Six Adhs are presented in this study. Adh1 is responsible for oxidation of ethanol. The cumulative FPKM of all Adhs was highest in the liver and duodenum, and markedly lower (about 25–35%) in the jejunum, ileum, and large intestine (Fig. 5B). The most abundantly expressed Adh in the liver and large intestine was Adh1, whereas in the small intestine, both Adh1 and 6a were most abundantly expressed. Most Adhs were highest expressed in the liver, except for Adh6a, which was almost exclusively expressed in the small intestine with highest expression in the duodenum.

Aldhs catalyze the oxidation and detoxification of aldehydes to carboxylic acids. There are 20 Aldhs in mice. Aldh2 is the major enzyme

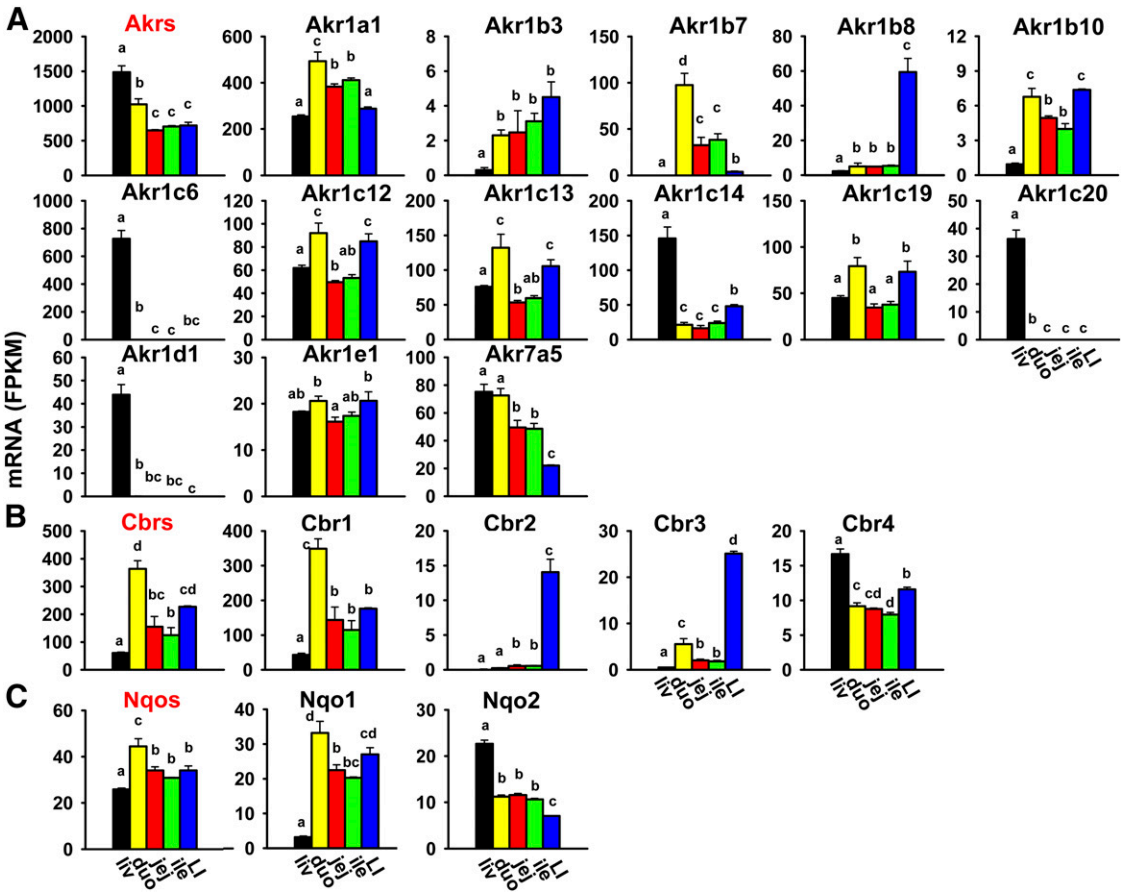


**Fig. 3.** Tissue distribution of Akr (A), Cbr (B), and Nqo (C) mRNAs in the liver and intestine. Data are presented as the mean FPKM ± S.E.M. of three individual animals. Any groups with the same letter are not different from each other (significance set at $p < 0.05$, one-way ANOVA followed by Duncan's post-hoc test). The tissue distribution of cumulative mRNAs of genes in each gene family is shown with red title. duo, duodenum; ile, ileum; jej, jejunum; LI, large intestine; liv, liver.

for the disposal of acetaldehyde generated during ethanol metabolism. The cumulative FPKM of all Aldhs was highest in the liver, medium in the small intestine (50% of liver), and lowest in the large intestine (Fig. 5C). The most abundantly expressed Aldhs in the liver were Aldh2 and 1a1; in the duodenum, Aldh1a1 and 1b1; in the jejunum and ileum, Aldh1b1, 1a1, and 9a1; and in the large intestine, Aldh2 and 1b1. Aldh3a1 was not expressed in the liver or intestine (Table 2). Half of these Aldhs were highest expressed in the liver, including Aldh1a1, 1a7, 1l1, 2, 3a2, 4a1, 5a1, 6a1, 7a1, and 8a1. The remaining Aldhs were highest expressed in the small intestine (duodenum: Aldh1a3, 3b1, 16a1, and 18a1; jejunum: Aldh1a2; ileum: Aldh1b1 and 9a1) and the large intestine (Aldh1l2 and 3b2).

Aldehyde oxidases (Aoxs) are molybdenum hydroxylases that oxidize aldehydes to their corresponding carboxylic acids with marked preference for aromatic aldehydes (e.g., benzaldehydes, tamoxifen aldehyde) (Parkinson et al., 2013). There are three Aox genes in the mouse genome. The cumulative FPKM of all Aoxs was highest in the liver and minimal in the intestine (Fig. 5C). The most abundantly expressed Aox in the liver was Aox3; in the jejunum, ileum, and large intestine, Aox1 was most abundantly expressed; whereas Aox1 and 3 were comparably expressed in the duodenum. Aox3l1 was not expressed in the liver or intestine (Table 2), whereas Aox1 and Aox3 were almost exclusively expressed in the liver (Fig. 5C).

Fmos, which are microsomal enzymes that require NADPH and oxygen similar to P450s, oxidize various xenobiotics, including nucleophilic nitrogen, sulfur, and phosphorus heteroatoms (Parkinson et al., 2013). There are five Fmos in the mouse genome. The cumulative FPKM of all Fmos was highest in the liver, medium in the three sections of the small intestine (approximately half of the FPKM in the liver), and lowest in the large intestine (Fig. 5D). The most abundantly expressed Fmos in the liver were Fmo5 and 1; in the small intestine, Fmo5 and 4; whereas four Fmos (Fmo1, 2, 4, and 5) had comparable expression in the large intestine. Fmo3 was not expressed in the liver or intestine (Table 2). Fmo1 and 5 were highest expressed in the liver, Fmo2 was highest expressed in the large intestine, and Fmo4 was highest expressed in the small intestine (Fig. 5D).

### Tissue Distribution of Phase II Enzymes in Liver and Intestine of Adult Male C57BL/6J Mice

Ugts are enzymes that transfer glucuronic acid from the cosubstrate UDP-glucuronic acid to various xenobiotics, which enhances their elimination and usually their detoxification. Twenty-one Ugt genes are presented in this study. The cumulative FPKM of all Ugts was highest in the liver, medium in the duodenum (about 50% of liver), and lowest and comparable levels in the jejunum, ileum, and large intestine (Fig. 6A). The most abundantly expressed Ugts in the liver were Ugt2b5, 2b36, and 2b1, whereas in the intestine, Ugt2b34 and 1a7c were the most abundantly expressed. Five Ugts were not expressed in the liver or intestine, including Ugt1a2, 1a10, 2a1, 2a2, and 8a (Table 2). Most Ugts were highest expressed in the liver (Ugt1a5, 1a6a, 1a6b, 1a9, 2a3, 2b1, 2b5, 2b35, 2b36, 2b37, 2b38, 3a1, and 3a2), whereas a few were highest expressed in the duodenum (Ugt1a1, 1a7c, and 2b34). Noticeably, many Ugts were almost exclusively expressed in the liver—namely, Ugt1a5, 2b1, 2b36, 2b37, 2b38, 3a1, and 3a2.

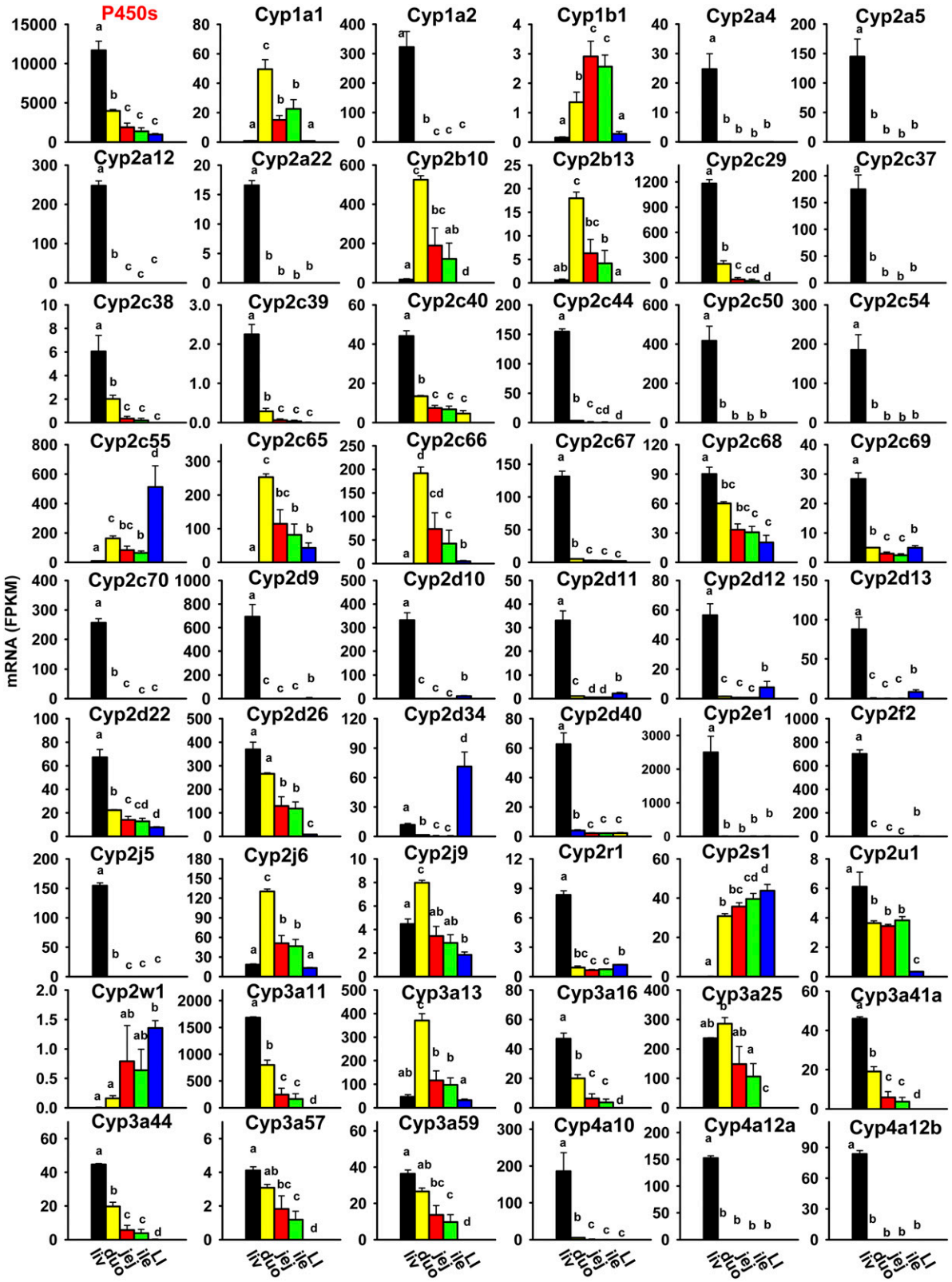


**Fig. 4.** Tissue distribution of some P450 mRNAs (Cyp1a1 to Cyp4a12b) in the liver and intestine. Data are presented as the mean FPKM ± S.E.M. of three individual animals. Any groups with the same letter are not different from each other (significance set at $p < 0.05$, one-way ANOVA followed by Duncan's post-hoc test). The tissue distribution of cumulative mRNAs of all P450s is shown with a red title. duo, duodenum; ile, ileum; jej, jejunum; LI, large intestine; liv, liver.

Sults are enzymes that are responsible for sulfonation of xenobiotics and endogenous substrates with the cosubstrate of 3′-phosphoadenosine-5′-phosphosulfate to produce a highly water-soluble sulfuric acid ester (Parkinson et al., 2013). Sixteen Sults are presented in this study. The cumulative FPKM of all Sults was highest in both the duodenum and large intestine, and lowest in the liver (less than 50% of

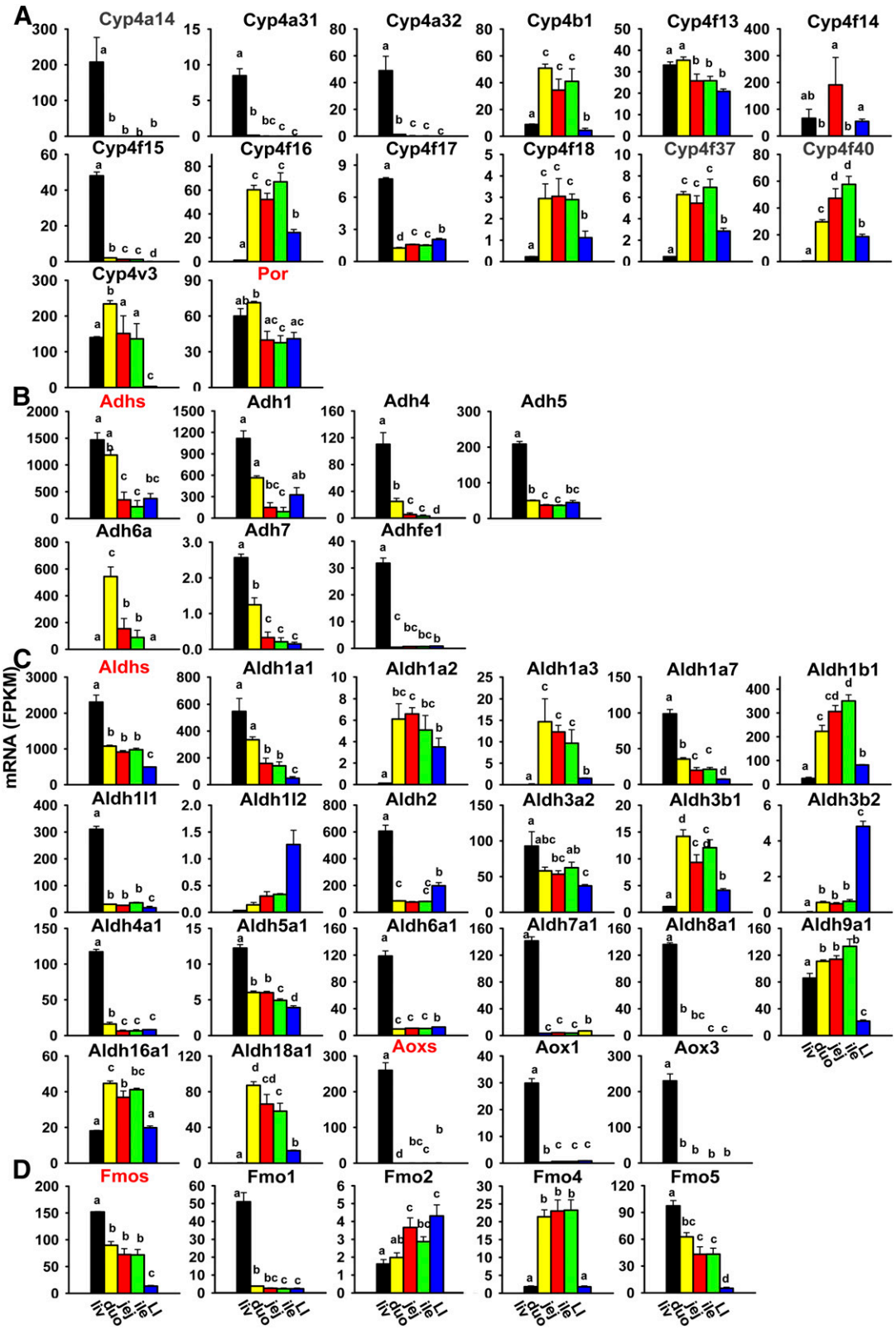


**Fig. 5.** Tissue distribution of other P450 (Cyp4a14 to Cyp4v3) and P450 (cytochrome) oxidoreductase (Por) (A), Adh (B), Aldh and Aox (C), and Fmo (D) mRNAs in liver and intestine. Data are presented as the mean FPKM ± S.E.M. of three individual animals. Any groups with the same letter are not different from each other (significance set at $p < 0.05$, one-way ANOVA followed by Duncan's post-hoc test). duo, duodenum; ile, ileum; jej, jejunum; LI, large intestine; liv, liver.

duodenum) (Fig. 6B). The most abundantly expressed Sults in the liver were Sult1a1 and 1d1; in the small intestine, Sult1d1, 1b1, and 2b1; and in the large intestine, Sult1a1, 1d1, and 1b1. Ten Sults were not expressed in the liver or intestine: Sult1c1, 1e1, 2a1, 2a2, 2a3, 2a4, 2a5, 2a7, 3a1, and 6b1 (Table 2). Sult5a1 was almost exclusively expressed in the liver, whereas Sult1d1 mRNA was highest in the

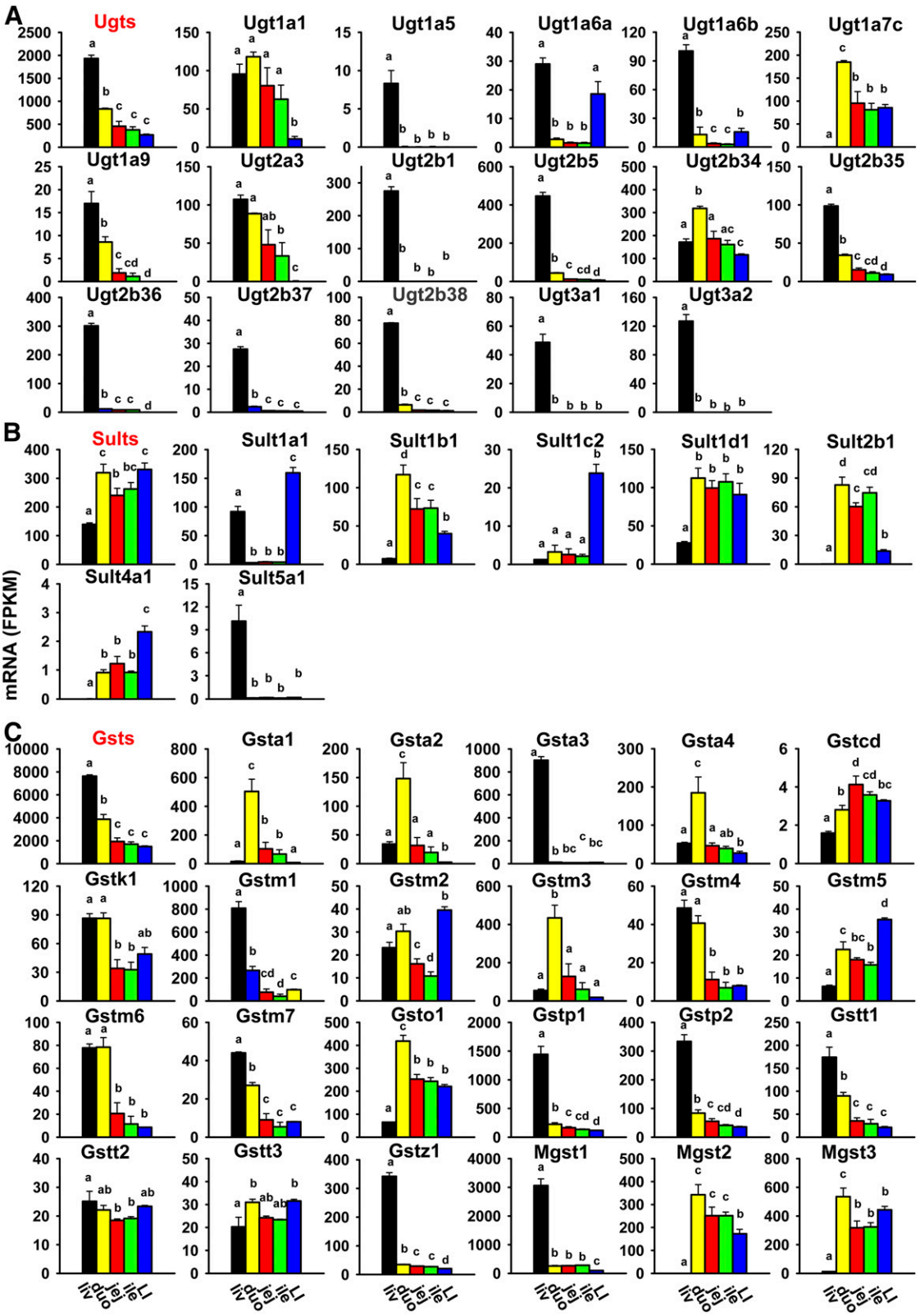


**Fig. 6.** Tissue distribution of Ugt (A), Sult (B), and Gst (C) mRNAs in the liver and intestine. Data are presented as the mean FPKM ± S.E.M. of three individual animals. Any groups with the same letter are not different from each other (significance set at $p < 0.05$, one-way ANOVA followed by Duncan's post-hoc test). The tissue distribution of cumulative mRNAs of genes in each gene family are shown with red title. duo, duodenum; ile, ileum; jej, jejunum; LI, large intestine; liv, liver.

intestine and much lower in the liver. Some were highest expressed in the small intestine (Sult1b1 and 2b1), and others were highest expressed in the large intestine (Sult1a1, 1c2, and 4a1).

Gsts catalyze the conjugation of electrophilic xenobiotics with the tripeptide glutathione as a cosubstrate, which is an important detoxification reaction (Parkinson et al., 2013). Cytosolic (class A, M, P,

T, Z, and O), mitochondrial (class K), and microsomal Gsts (Mgsts) are expressed in mice, which include 25 Gst genes. The cumulative FPKM of all Gsts was highest in the liver, medium in the duodenum (about 50% of liver), and lowest in the jejunum, ileum, and large intestine (Fig. 6C). The most abundantly expressed Gsts in the liver were Mgst1 and Gstp1, a3, and m1; in the duodenum, Mgst3 and Gsta1, m3, and o1; and in the jejunum, ileum, and large intestine, Mgst3, 1, 2, and Gsto1. Gsto2 and t4 were not expressed in the liver or intestine (Table 2). Some Gsts were highest expressed in the liver (Gsta3, m1, m7, p1, p2, t1, z1, and Mgst1), and others were highest expressed in the duodenum (Gsta1, a2, a4, m3, o1, and Mgst2 and 3). Some Gsts were highest expressed in both the liver and duodenum (Gstk1, m4, and m6). A few Gsts were highest expressed in the jejunum (Gst, C-terminal domain containing or Gstcd) or large intestine (Gstm2 and m5). Gstt2 and t3 had less divergent expression among tissues. Noticeably, some were almost exclusively expressed in the liver (Gsta3) or small intestine (Gsta1).

Unlike most phase II conjugation reactions, methylation and acetylation generally decrease the water solubility of xenobiotics and mask functional groups that might otherwise be metabolized by other conjugating enzymes. The cosubstrates for methylation and acetylation are *S*-adenosylmethionine and acetyl-CoA, respectively. Catechol *O*-methyltransferase catalyzes the methylation of many phenolic compounds. Catechol *O*-methyltransferase mRNA was highest in the liver and much lower in all sections of the intestine (Fig. 7A). Arsenic (+3 oxidation state) methyltransferase methylates inorganic arsenic to form methylarsonic and dimethylarsonic acids, which are more cytotoxic and genotoxic than arsenate and arsenite (Wood et al., 2006). Arsenic (+3 oxidation state) methyltransferase mRNA was highest in the small intestine, slightly lower in the large intestine, and lowest in the liver (Fig. 7A). Thiopurine *S*-methyltransferase plays an important role in the methylation and detoxification of some thiopurine drugs. Thiopurine *S*-methyltransferase mRNA was highest in the liver and much lower in all sections of the intestine (Fig. 7A). Acetylation, catalyzed by the arylamine *N*-actyltransferases Nat1, 2, and 3, is a major biotransformation pathway for xenobiotics containing an aromatic amine or a hydrazine group. Nat1 and 3 were not expressed in the liver or intestine (Table 2). Nat2 mRNA was highest in all sections of the intestine at comparable levels, and was lowest in the liver (about 50% of duodenum) (Fig. 7A).

In addition to the conjugation reactions discussed earlier, endobiotic chemicals and xenobiotics can also undergo conjugation with amino acids. Bile acid–CoA ligase (Slc27a5) and bile acid–CoA:amino acid *N*-acyltransferase catalyze reactions of bile acid conjugation with glycine and taurine. Glycine-*N*-acyltransferase is responsible for glycine conjugation and detoxification of xenobiotics, such as salicylic acid, benzoic acid, and methylbenzoic acid (Badenhorst et al., 2012). Bile acid–CoA ligase, bile acid–CoA:amino acid *N*-acyltransferase, and glycine-*N*-acyltransferase were almost exclusively expressed in the liver (Fig. 7A).

Several enzymes are involved in the synthesis of cosubstrates for phase II conjugation. UDP-glucose pyrophosphorylase 2 catalyzes the synthesis from glucose-1-phosphate to UDP-glucose, and UDP-glucose 6-dehydrogenase converts UDP-glucose to UDP-glucuronic acid, which is the cosubstrate for UDP-glucuronidation. UDP-glucose pyrophosphorylase 2 mRNA was highest in the liver, medium in the large intestine, and lowest in all sections of the small intestine, whereas UDP-glucose 6-dehydrogenase mRNA was higher in the large intestine and duodenum, and lower in the liver, jejunum, and ileum (Fig. 7B).

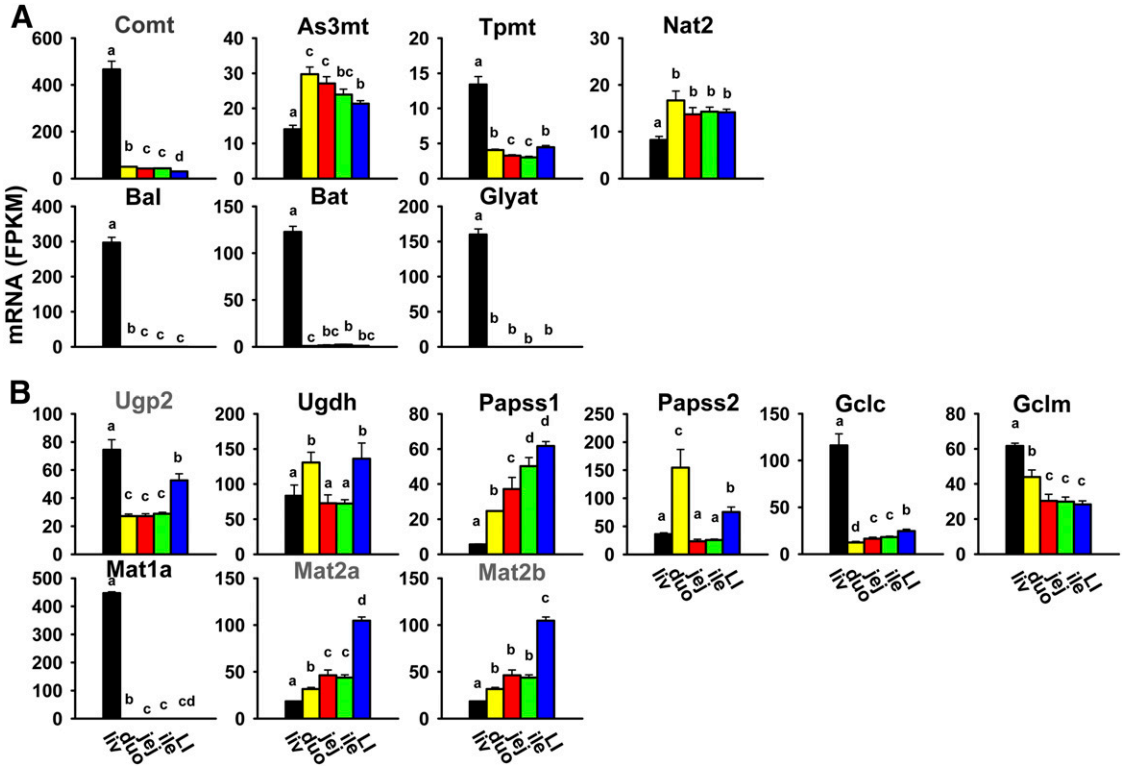


**Fig. 7.** Tissue distribution of mRNAs of enzymes responsible for methylation, acetylation, and amino acid conjugation (A), and synthesis of cosubstrates for phase II conjugation reactions in the liver and intestine (B). Data are presented as the mean FPKM ± S.E.M. of three individual animals. Any groups with the same letter are not different from each other (significance set at $p < 0.05$, one-way ANOVA followed by Duncan's post-hoc test). $As_3$mt, arsenic (+3 oxidation state) methyltransferase; Bal, bile acid–CoA ligase; Bat, bile acid–CoA:amino acid *N*-acyltransferase; Comt, catechol *O*-methyltransferase; duo, duodenum; Gclc, glutamate-cysteine ligase catalytic subunit; Gclm, glutamate-cysteine ligase modifier subunit; Glyat, glycine-*N*-acyltransferase; ile, ileum; jej, jejunum; LI, large intestine; liv, liver; Tpmt, thiopurine *S*-methyltransferase; Ugdh, UDP-glucose 6-dehydrogenase; Ugp2, UDP-glucose pyrophosphorylase 2.

3′-Phosphoadenosine 5′-phosphosulfate synthase 1 (Papss1) and Papss2 catalyze the synthesis of 3′-phosphoadenosine-5′-phosphosulfate, the sulfate donor for all Sults; Papss1 mRNA gradually increased from the liver, duodenum, jejunum, and ileum to the large intestine, whereas Papss2 mRNA was highest in the duodenum, medium in the large intestine, and lowest in the liver, jejunum, and ileum (Fig. 7B). Glutamate-cysteine ligase catalytic and modifier subunits catalyze the synthesis of glutathione, which is the cosubstrate for all Gsts. Glutamate-cysteine ligase catalytic subunit mRNA was highest in the liver and much lower in all sections of the intestine, and glutamate-cysteine ligase modifier subunit mRNA gradually decreased from the liver and small intestine to large intestine (Fig. 7B). Methionine adenosyltransferases (Mat enzymes) are responsible for the synthesis of the common methyl donor *S*-adenosylmethionine. Mat1a was almost exclusively expressed

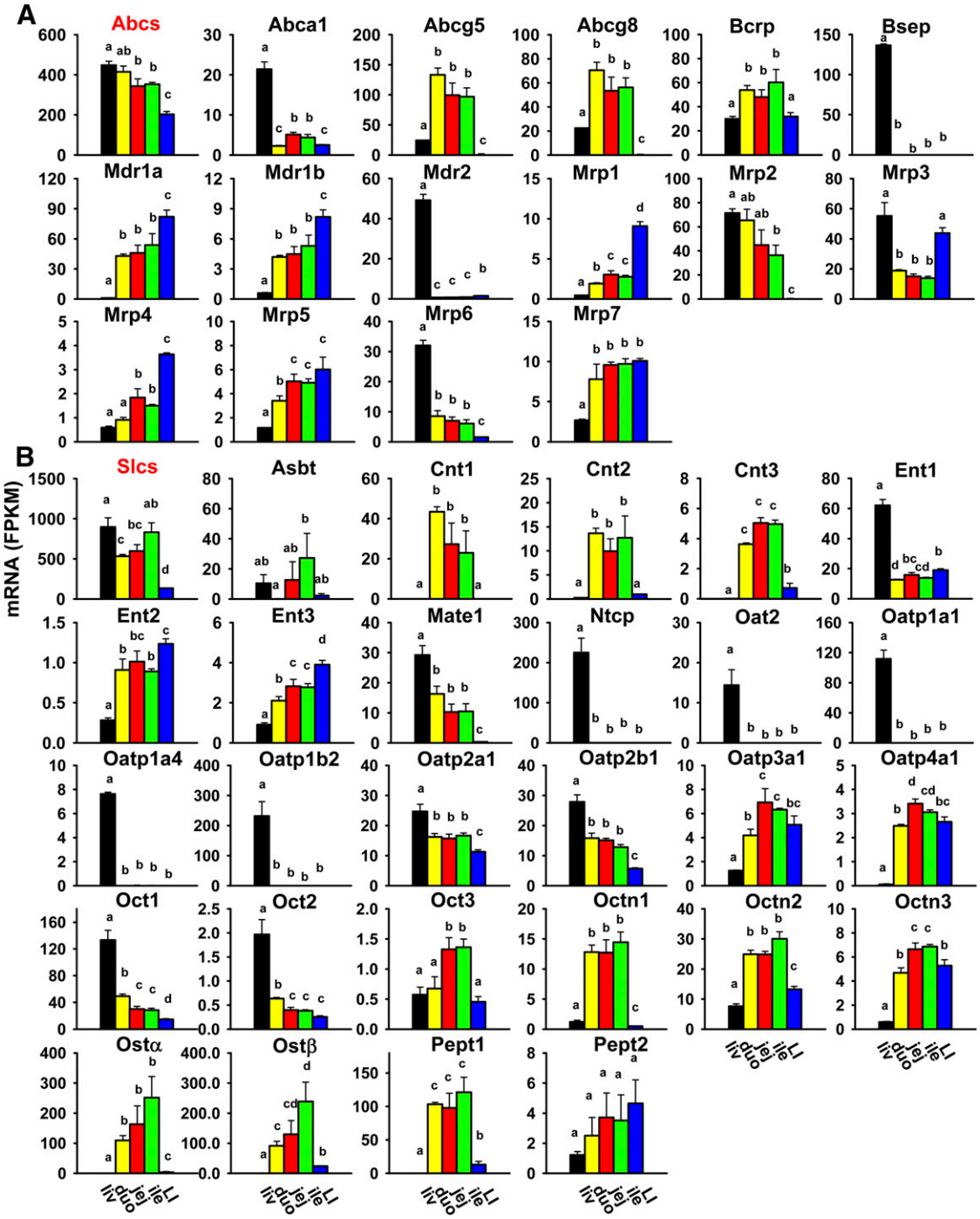


**Fig. 8.** Tissue distributio(n of mRNAs of Abc (A) and Slc xenobiotic transporters (B) in the liver and intestine. Data are presented as the mean FPKM ± S.E.M. of three individual animals. Any groups with the same letter are not different from each other (significance set at $p < 0.05$, one-way ANOVA followed by Duncan's post-hoc test). The tissue distribution of cumulative mRNAs of all Abc and Slc drug transporters are shown with a red title. Abst, apical sodium-dependent bile acid transporter; Cnt, concentrative nucleoside transporter; duo, duodenum; Ent, equilibrative nucleoside transporter; ile, ileum; jej, jejunum; LI, large intestine; liv, liver; Mdr, multidrug resistance protein; Mrp, multidrug resistance-associated protein; Ntcp, $Na^+$-taurocholate cotransporting polypeptide; Oat, organic anion transporter; Oatp, organic anion transporting polypeptide; Oct, organic cation transporter; Octn, organic cation/carnitine transporter.

in the liver, whereas Mat2a and 2b mRNAs were highest in the large intestine, medium in the small intestine, and lowest in the liver (Fig. 7B).

### Tissue Distribution of Xenobiotic Transporters in Liver and Intestine of Adult Male C57BL/6J Mice

Transporters with importance in xenobiotic transport were characterized, including 39 Slcs and 17 Abc transporters. Most of the Slc transporters are uptake transporters [34 Slcs, including 15 solute carrier organic anions (Slcos)], but they also include a few efflux transporters, including multidrug and toxin extrusion transporters (Mate1/Slc47a1 and Mate2/Slc47a2) and organic solute transporters (Ost$\alpha$/Slc51a and Ost$\beta$/Slc51b). Eleven uptake transporters (Oat1/Slc22a6, Oat3/Slc22a8, urate transporter 1 Urat1/Slc22a12, Oatp/Slco1a5, 1a6, 1c1, 4c1, 5a1, 6b1, 6c1, and 6d1) and three efflux transporters (Mate2, Mrp8/Abcc8, and Mrp9/Abcc12) were not expressed in the liver or intestine (Table 2). The uptake transporters with the most abundant expression in the liver were Ntcp/Slc10a1 and Oatp1b2/Slco1b2; in the small intestine, Pept1/Slc15a1; and in the large intestine, Ent1/Slc29a1, Octn2/Slc22a5, Oatp2a1/Slco2a1, and Pept1. The efflux transporters with the most abundant expression in the liver were bile salt export pump (Bsep)/Abcb11, Mrp2/Abcc2, and Mrp3/Abcc3; in the small intestine, Abcg5, Ost$\alpha$, and Ost$\beta$; and in the large intestine, Mdr1a/Abcb1a.

The cumulative FPKM of all Abc transporters gradually decreased from the liver and small intestine to the large intestine (Fig. 8A). Some Abcs were highest expressed in the liver (Abca1, Bsep, Mdr2/Abcb4, Mrp/Abcc2, 3, and 6), some were highest expressed in the duodenum (Abcg5 and 8), and others were highest expressed in the large intestine (Mdr1a, 1b, Mrp/Abcc1, 4, and 5). Breast cancer resistance protein (Bcrp)/Abcg2 was highest expressed in the ileum. Mrp7/Abcc10 mRNA was lowest in the liver and higher in the small and large intestine. Noticeably, Bsep and Mdr2 were almost exclusively expressed in the liver.

The cumulative FPKM of all Slc transporters was highest in the liver and ileum, medium in the duodenum and jejunum, and lowest in the large intestine (Fig. 8B). Some were highest expressed in the liver (Ent1, Mate1, Ntcp, Oat2/Slc22a7, Oatp1a1/Slco1a1, Oatp1a4/Slco1a4, Oatp1b2/Slco1b2, Oatp2a1/Slco2a1, Oatp2b1/Slco2b1, Oct1/Slc22a1, and Oct2/Slc22a2), some were highest expressed in the small intestine (Asbt/Slc10a2, Cnt1/Slc28a1, Cnt2/Slc28a2, Cnt3/Slc28a3, Oatp3a1/Slco3a1, Oatp4a1/Slco4a1, Oct3/Slc22a3, Octn1/Slc22a4, Octn2/Slc22a5, Octn3/Slc22a21, Ost$\alpha$, Ost$\beta$, and Pept1), whereas others were highest expressed in the large intestine (Ent2/Slc29a2, Ent3/Slc29a3, and Pept2/Slc15a2). Noticeably, some Slcs were almost exclusively expressed in the liver (Ntcp, Oat2, Oatp1a1, 1a4, and 1b2) or small intestine (Cnt1, Cnt2, and Ost$\alpha$).

### Tissue Distribution of Xenobiotic-Related Transcription Factors in Liver and Intestine of Adult Male C57BL/6J Mice

Various TFs, such as the aryl hydrocarbon receptor (AhR), constitutive androstane receptor (CAR/Nr1i3), farnesoid X receptor (FXR/Nr1h4), hepatocyte nuclear factors (HNF1$\alpha$ and HNF4$\alpha$/Nr2a1), peroxisome proliferator-activated receptor $\alpha$ (PPAR$\alpha$/Nr1c1), pregnane X receptor (PXR/Nr1i2), retinoid X receptors (RXR$\alpha$/Nr2b1, RXR$\beta$/Nr2b2, and RXR$\gamma$/Nr2b3), and nuclear factor erythroid 2-related factor 2 (Nrf2), are involved in the expression of xenobiotic-metabolizing enzymes and transporters. The most abundantly expressed transcription factor in the liver was HNF4$\alpha$; in the small intestine, HNF4$\alpha$ and Nrf2; and in the large intestine, HNF4$\alpha$, RXR$\alpha$, and Nrf2. CAR, RXR$\alpha$, and RXR$\gamma$ were highest expressed in the large intestine (Fig. 9). FXR was highest expressed in both the liver and ileum. PPAR$\alpha$ and PXR were highest expressed in the liver, whereas Nrf2 mRNA was lowest in the liver and higher in both the small and large intestine. RXR$\beta$ mRNA was lowest in the large intestine and higher in the liver and small intestine. AhR, HNF1$\alpha$, and HNF4$\alpha$ had less divergent expression among tissues.

## Discussion

The present study has provided a comprehensive quantitative analysis of mRNA expression profiles of all major XPGs in various sections of the intestine compared with the liver of male mice. Specifically, this study has illustrated that the expression of XPGs in male mice displays high tissue-divergent patterns. The majority of the XPGs (254 out of 304) have different expression among tissues, which can be partitioned into liver-predominant, small intestine–predominant, and large intestine–predominant expression patterns (Fig. 1). Over half of the differentially expressed XPGs (136 out of 254) are expressed highest in the liver. The most abundantly expressed gene in the liver is Mgst1; in the duodenum, Cyp3a11; in the jejunum and ileum, Ces2e; and in the large intestine, Cyp2c55 (Table 3).

The present findings of XPG expression in the liver are consistent with previous RNA-Seq reports in adult male mice (Cui et al., 2012; Peng et al., 2012, 2013; Lu et al., 2013). The present study is novel because it has unveiled the true quantification of XPGs in various sections of the

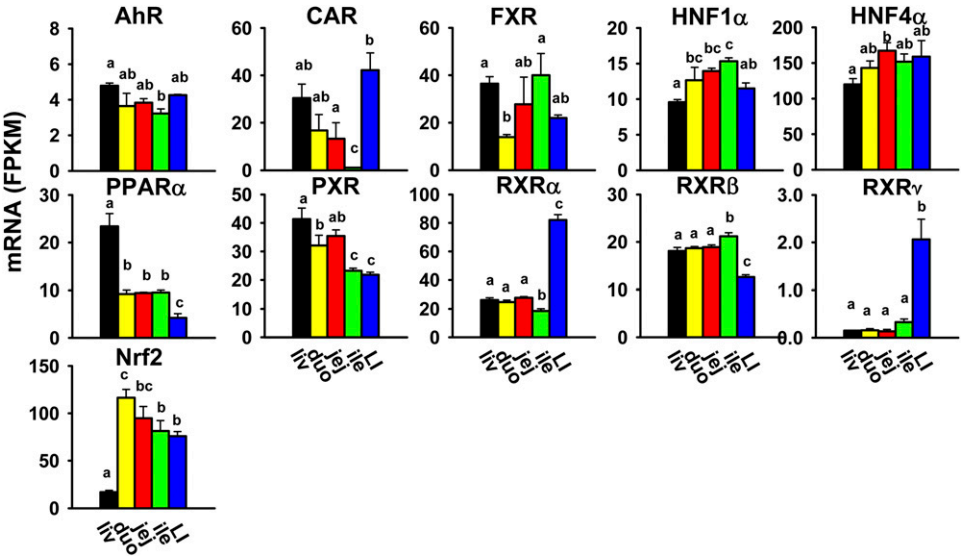


**Fig. 9.** Tissue distribution of mRNAs of genes encoding xenobiotic-related transcription factors in the liver and intestine. Data are presented as the mean FPKM ± S.E.M. of three individual animals. Any groups with the same letter are not different from each other (significance set at $p < 0.05$, one-way ANOVA followed by Duncan's post-hoc test). duo, duodenum; ile, ileum; jej, jejunum; LI, large intestine; liv, liver.

TABLE 3

List of top 10 abundantly expressed XPGs in each tissue

| Tissue | Gene Name | FPKM |
|---|---|---|
| Liver | Mgst1 | 3062 |
| | Cyp2e1 | 2502 |
| | Cyp3a11 | 1686 |
| | Gstp1 | 1442 |
| | Cyp2c29 | 1180 |
| | Adh1 | 1114 |
| | Ces1c | 925.2 |
| | Gsta3 | 902.7 |
| | Ces3a | 879.0 |
| | Gstm1 | 807.3 |
| Duodenum | Cyp3a11 | 798.8 |
| | Ces2e | 778.5 |
| | Adh1 | 564.0 |
| | Adh6a | 542.8 |
| | Mgst3 | 533.7 |
| | Cyp2b10 | 525.6 |
| | Gsta1 | 502.9 |
| | Akr1a1 | 493.8 |
| | Gstm3 | 434.3 |
| | Gsto1 | 418.7 |
| Jejunum | Ces2e | 422.0 |
| | Akr1a1 | 383.2 |
| | Mgst3 | 317.3 |
| | Aldh1b1 | 306.4 |
| | Mgst1 | 267.7 |
| | Gsto1 | 252.8 |
| | Mgst2 | 251.1 |
| | Cyp3a11 | 244.3 |
| | Cyp4f14 | 191.0 |
| | Cyp2b10 | 189.5 |
| Ileum | Ces2e | 459.6 |
| | Akr1a1 | 411.3 |
| | Aldh1b1 | 350.5 |
| | Mgst3 | 323.7 |
| | Mgst1 | 281.3 |
| | Ost$\alpha$ | 251.4 |
| | Mgst2 | 251.3 |
| | Gsto1 | 243.3 |
| | Ost$\beta$ | 238.7 |
| | Ces2a | 180.8 |
| Large intestine | Cyp2c55 | 512.3 |
| | Mgst3 | 442.5 |
| | Adh1 | 324.6 |
| | Akr1a1 | 287.6 |
| | Gsto1 | 220.8 |
| | Aldh2 | 197.2 |
| | Cbr1 | 176.3 |
| | Mgst2 | 172.4 |
| | Sult1a1 | 159.5 |
| | HNF4$\alpha$ | 158.8 |

intestine, in comparison with that in liver. Previous studies have characterized the tissue-specific mRNA expression of many XPGs in rodents mostly using conventional mRNA profiling tools (Table 4). The present study has provided novel knowledge on the tissue distribution of more XPGs, such as many non-P450 phase I enzymes (Ephxs, Cbrs, Nqos, Adhs, and Aoxs) as well as other XPGs that were previously underinvestigated due to either less appreciation of their importance for processing drugs (Akr1b10, Aldh1l1, 3b2, 5a1, 16a1, Cyp2d13, 2j11, Gstcd, and Gstm7) or the technical challenges of designing specific primers for genes with high DNA sequence similarity (Ugt2b5/37/38, Ugt2a1/2, Ugt3a1/2, Gsta1/2, and Gstp1/2). The present study has also provided valuable information on XPG expression in various sections of the intestine (three sections of the small intestine as well as the large intestine) in comparison with the previous microarray study of the small intestine as a whole (Thorrez et al., 2008). One is able to compare the abundance of various XPGs from the present RNA-Seq study, whereas this is not possible in a microarray study due to different probe hybridization efficiencies for various genes. Findings between the present RNA-Seq study and previous publications have been compared in detail in the following four paragraphs.

Most of our findings on the tissue distribution of many phase I enzymes (Pons, Akrs, P450s, Aldhs, and Fmos) are consistent with previous reports; however, several discrepancies are discussed here. For Pons, the present study has shown that both Pon2 and 3 mRNAs are lower in the jejunum and ileum than in the large intestine, in contrast to the previous report of similar levels (Cheng and Klaassen, 2012). For Akrs, the mRNAs of Akr1a1/1a4, 1b3, 1c12, 1c13, 1c19, and 1e1 in certain tissue(s) in the present study are not fully consistent with a previous report (Pratt-Hyatt et al., 2013). For P450s, there are some inconsistencies between the present study and a previous report (Renaud et al., 2011) on Cyp2b13, 2d12, 2j9, 4f14, 4f37, and 4v3. For Aldhs, the data on Aldh3a2 and 3b1 in the present study are slightly different from a previous report (Alnouti and Klaassen, 2008). For Fmos, the present study is novel because it has identified that the expression of Fmos in the intestine is section-specific, which was not reported before (Janmohamed et al., 2004). Fmo3 is not expressed in the liver or intestine of mice (Table 2), whereas Fmo3 is the major drug-metabolizing Fmo in human liver (Cashman and Zhang, 2006). All of the previously discussed discrepancies are likely due to the low fidelity to quantify lowly expressed genes by conventional methods, or species differences in tissue distribution of some XPGs. More importantly, this study has identified the most abundantly expressed gene within the same family. For example, Akr1c6 is the most abundantly expressed Akr in the liver, which correlates with its critical roles in steroid biogenesis, xenobiotic metabolism, and bile acid synthesis. The most abundantly expressed Aldh in the liver is Aldh2, consistent with its major role in ethanol metabolism and detoxification. Cyp2e1 (for many halogenated alkanes and nitrosamines as well as ethanol) and Cyp3a11 (for steroid hormones and a wide range of xenobiotics, including drugs from numerous therapeutic classes; CYP3A is responsible for the metabolism of about 50% of drugs in humans) are well known for their roles in xenobiotic metabolism, and it is noteworthy that the most abundantly expressed P450 in the liver is Cyp2e1, and in the small intestine, Cyp3a11. The finding that Cyp2c55 (synthesis of an arachidonic acid metabolite important for ion transport and renal vascular tone, and mediation of triazole fungicide–induced hepatotoxicity) is the most abundantly expressed P450 in the large intestine is very interesting, the mechanism or function of which needs to be further investigated.

Our current findings for Ugts, Sults, and Gsts are largely consistent with previous reports in mice from our laboratory using conventional mRNA quantification methods (Alnouti and Klaassen, 2006; Buckley and Klaassen, 2007; Knight et al., 2007), with the exception of Ugt1a7c, Sult4a1, 5a1, and Papss1 (Figs. 6 and 7). The discrepancies possibly result from different experiment conditions, such as vendors of mice, mice chows, and RNA-quantification methods. Compared with data in rats (Dunn and Klaassen, 1998; Shelby et al., 2003), species differences in tissue-specific expression of Ugts, Sults, and Gsts were observed. The present study is generally consistent with a recent RNA-Seq study of all phase II enzymes in the small intestine of adult mice (Lu et al., 2013), and has added new knowledge to the field by profiling phase II enzymes in all three sections of the small intestine as well as the large intestine.

The present findings on xenobiotic transporters are generally consistent with previous reports on mice from our and others' laboratories (Yu et al., 2002; Buist and Klaassen, 2004; Ballatori et al., 2005; Cheng et al., 2005; Tanaka et al., 2005; Alnouti et al., 2006; Lu and Klaassen, 2006; Lickteig et al., 2008; Cheng and Klaassen, 2009; Cui et al., 2009), with the exception of Bcrp, Mdr1b, Mrp1-5, Oatp2a1, and Oatp2b1 (Fig. 8). Compared with data in rats (Brady et al., 2002;

TABLE 4

List of previous publications on the tissue distribution of XPG mRNA expression

| Gene Family | Species | Gender | Number of Tissues | Assay | References |
|---|---|---|---|---|---|
| Ces | Mice | M | 16 | RT-qPCR | Jones et al., 2013 |
| Pon | Mice | M; F | 12 | bDNA assay | Cheng and Klaassen, 2012 |
| Akr | Mice | M; F | 12 | RT-qPCR | Pratt-Hyatt et al., 2013 |
| P450 | Mice | M; F | 13 | Multiplex suspension assay; RT-qPCR | Renaud et al., 2011 |
| Aldh | Mice | M; F | 14 | bDNA assay | Alnouti and Klaassen, 2008 |
| Fmo | Mice | M | 4 | RNase protection | Janmohamed et al., 2004 |
| Ugt | Mice | M; F | 12 | bDNA assay | Buckley and Klaassen, 2007 |
| Ugt | Rats | M; F | 36 | bDNA assay | Shelby et al., 2003 |
| Sult | Mice | M; F | 14 | bDNA assay | Alnouti and Klaassen, 2006 |
| Sult | Rats | M; F | 12 | Northern blot | Dunn and Klaassen, 1998 |
| Gst | Mice | M; F | 14 | bDNA assay | Knight et al., 2007 |
| All phase II | Mice | M | 3 | RNA-Seq | Lu et al., 2013 |
| Abca1; Asbt | Mice | M; F | 13 | bDNA assay | Cheng and Klaassen, 2009 |
| Abcg5, 8 | Mice | M; F | 2 | Northern blot | Yu et al., 2002 |
| Bcrp | Mice; rats | M; F | 20; 18 | bDNA assay | Tanaka et al., 2005 |
| Mdr | Mice | M; F | 12 | bDNA assay | Cui et al., 2009 |
| Mrp | Mice | M; F | 12 | bDNA assay | Maher et al., 2005 |
| Cnt; Ent | Mice; rats | M; F | 19 | bDNA assay | Lu et al., 2004 |
| Mate | Mice | M; F | 13 | bDNA assay | Lickteig et al., 2008 |
| Oat | Mice | M; F | 6 | bDNA assay | Buist and Klaassen, 2004 |
| Oatp | Mice | M; F | 11 | bDNA assay | Cheng et al., 2005 |
| Oct | Mice | M; F | 14 | bDNA assay | Alnouti et al., 2006 |
| Ost$\alpha$, $\beta$ | Mice; rats | M | 6 | Northern blot; RT-qPCR | Ballatori et al., 2005 |
| Pept | Mice; rats | M; F | 19 | bDNA assay | Lu and Klaassen, 2006 |
| Mdr1a, 1b | Rats | M | 10 | bDNA assay | Brady et al., 2002 |
| Mrp1-3 | Rats | M | 10 | bDNA assay | Cherrington et al., 2002 |
| Mrp4 | Rats | M; F | 11 | bDNA assay | Chen and Klaassen, 2004 |
| Mrp5, 6 | Rats | M; F | 10 | bDNA assay | Maher et al., 2006 |
| Oatp1-5 | Rats | M; F | 10 | bDNA assay | Li et al., 2002 |
| Oct | Rats | M | 20 | bDNA assay | Slitt et al., 2002 |
| NRs | Mice | M; F | 39 | RT-qPCR | Bookout et al., 2006 |
| TFs | Mice | M; F | 14 | bDNA assay | Petrick and Klaassen, 2007 |
| All XPGs | Mice | M | 22 | Microarray | Thorrez et al., 2008 |

bDNA, branched-DNA; F, female; M, male; NRs, nuclear receptors; RT-qPCR, reverse-transcription quantitative real-time polymerase chain reaction.

Cherrington et al., 2002; Li et al., 2002; Slitt et al., 2002; Chen and Klaassen, 2004; Lu et al., 2004; Ballatori et al., 2005; Tanaka et al., 2005; Lu and Klaassen, 2006; Maher et al., 2006), species differences in tissue-specific expression of Bcrp, Mdr1a, 1b, Mrp2, 3, Cnt1–3, Oct1, Pept1, and Pept2 are observed. More importantly, this study reveals the xenobiotic transporters with the highest mRNA levels in each tissue. The most abundantly expressed uptake transporters in the liver are Ntcp (for conjugated bile acids) and Oatp1b2 (for unconjugated bile acids, phalloidin, and statins); in the small intestine, Pept1 (for di- and tripeptides, such as glycylsarcosine, as well as cephalexin); and in the large intestine, Ent1 (for nucleosides, such as anticancer and antiviral drugs). The most abundantly expressed efflux transporter in the liver is Bsep (for conjugated bile acids); in the small intestine, Abcg5 (for sterols), Ost$\alpha$, and Ost$\beta$ (for bile acids); and in the large intestine, Mdr1a (for various drugs and other chemicals).

The present study provides crucial information on mRNA abundance of various xenobiotic-related TFs in the liver and intestine of male mice. CAR and PXR, the two well characterized xenobiotic sensors, have high expression in the liver (Fig. 9), and CAR also has unexpectedly high expression in the large intestine. Previous reports on CAR and PXR (Bookout et al., 2006; Petrick and Klaassen, 2007) showed discrepant results and, moreover, were not fully consistent with the present study (Fig. 9). This is likely due to the differences in genetic backgrounds of mice, housing conditions, chows, and RNA-quantification method, and implicates the necessity of further investigation. We and others (Bookout et al., 2006) have shown that FXR has a high expression in the liver and ileum, which correlates with its regulatory role in bile acid homeostasis and enterohepatic circulation. Noticeably, Nrf2, the master regulator of the cellular defense system against oxidative stress, has much higher expression in the intestine than the liver, as previously reported (Petrick and Klaassen, 2007). In line with the recent notion of Nrf2 as a multiorgan protector (Lee et al., 2005), this finding will likely attract increasing attention to the role of Nrf2 in oxidative stress response and carcinogenesis in the intestine. The findings on AhR and PPAR$\alpha$ in the present study are generally consistent with a previous report (Petrick and Klaassen, 2007). Interestingly, HNF4$\alpha$ accounts for $>$40% of total transcripts of all of these xenobiotic-related TFs in the liver as well as all sections of the intestine, which correlates with its role as a master regulator of the basal expression of many genes involved in differentiation and proliferation, intermediary and xenobiotic metabolism, as well as inflammation (Li et al., 2000; Gonzalez, 2008; Babeu and Boudreau, 2014).

Protein levels and activities of XPGs were not determined in this study due to the extensive workload and the technical obstacle that specific antibodies, substrates, and inhibitors for many XPGs are not available. Thus, caution should be taken in the extrapolation of mRNA expression of XPGs to their protein expression and function. Technology breakthroughs in proteomics and metabolomics are essential to conduct genome-scale comparative studies to identify the sets of genes whose expression is mainly regulated at the post-transcriptional level. Furthermore, marked sex differences in the expression of many XPGs are well known (Waxman and Holloway, 2009; Fu et al., 2012), and thus it will be equally important to determine the XPG expression profiles in the liver and intestine of female mice in the future.

In conclusion, the present study is the first to provide true quantification of mRNA abundance of all major XPGs in various sections of mouse intestine as well as liver. Such knowledge will shed light on tissue-specific biotransformation and toxicity of drugs and other

xenobiotics and provide important resources for the investigation and interpretation of tissue-specific expression of XPGs in humans.

### Acknowledgments

The authors thank Clark Bloomer from the KUMC genomic sequencing facilities for technical assistance on RNA-Seq.

### Authorship Contributions

*Participated in research design:* Selwyn, Cui, Klaassen.
*Conducted experiments:* Selwyn, Cui.
*Performed data analysis:* Fu, Cui, Klaassen.
*Wrote or contributed to the writing of the manuscript:* Fu, Cui, Klaassen.

### References

Alnouti Y and Klaassen CD (2006) Tissue distribution and ontogeny of sulfotransferase enzymes in mice. *Toxicol Sci* **93**:242–255.
Alnouti Y and Klaassen CD (2008) Tissue distribution, ontogeny, and regulation of aldehyde dehydrogenase (Aldh) enzymes mRNA by prototypical microsomal enzyme inducers in mice. *Toxicol Sci* **101**:51–64.
Alnouti Y, Petrick JS, and Klaassen CD (2006) Tissue distribution and ontogeny of organic cation transporters in mice. *Drug Metab Dispos* **34**:477–482.
Babeu JP and Boudreau F (2014) Hepatocyte nuclear factor 4-alpha involvement in liver and intestinal inflammatory networks. *World J Gastroenterol* **20**:22–30.
Badenhorst CP, Jooste M, and van Dijk AA (2012) Enzymatic characterization and elucidation of the catalytic mechanism of a recombinant bovine glycine N-acyltransferase. *Drug Metab Dispos* **40**:346–352.
Ballatori N, Christian WV, Lee JY, Dawson PA, Soroka CJ, Boyer JL, Madejczyk MS, and Li N (2005) OSTalpha-OSTbeta: a major basolateral bile acid and steroid transporter in human intestinal, renal, and biliary epithelia. *Hepatology* **42**:1270–1279.
Bookout AL, Jeong Y, Downes M, Yu RT, Evans RM, and Mangelsdorf DJ (2006) Anatomical profiling of nuclear receptor expression reveals a hierarchical transcriptional network. *Cell* **126**: 789–799.
Brady JM, Cherrington NJ, Hartley DP, Buist SC, Li N, and Klaassen CD (2002) Tissue distribution and chemical induction of multiple drug resistance genes in rats. *Drug Metab Dispos* **30**: 838–844.
Buckley DB and Klaassen CD (2007) Tissue- and gender-specific mRNA expression of UDP-glucuronosyltransferases (UGTs) in mice. *Drug Metab Dispos* **35**:121–127.
Buist SC and Klaassen CD (2004) Rat and mouse differences in gender-predominant expression of organic anion transporter (Oat1-3; Slc22a6-8) mRNA levels. *Drug Metab Dispos* **32**:620–625.
Cashman JR and Zhang J (2006) Human flavin-containing monooxygenases. *Annu Rev Pharmacol Toxicol* **46**:65–100.
Chen C and Klaassen CD (2004) Rat multidrug resistance protein 4 (Mrp4, Abcc4): molecular cloning, organ distribution, postnatal renal expression, and chemical inducibility. *Biochem Biophys Res Commun* **317**:46–53.
Cheng X and Klaassen CD (2009) Tissue distribution, ontogeny, and hormonal regulation of xenobiotic transporters in mouse kidneys. *Drug Metab Dispos* **37**:2178–2185.
Cheng X and Klaassen CD (2012) Hormonal and chemical regulation of paraoxonases in mice. *J Pharmacol Exp Ther* **342**:688–695.
Cheng X, Maher J, Chen C, and Klaassen CD (2005) Tissue distribution and ontogeny of mouse organic anion transporting polypeptides (Oatps). *Drug Metab Dispos* **33**:1062–1073.
Cherrington NJ, Hartley DP, Li N, Johnson DR, and Klaassen CD (2002) Organ distribution of multidrug resistance proteins 1, 2, and 3 (Mrp1, 2, and 3) mRNA and hepatic induction of Mrp3 by constitutive androstane receptor activators in rats. *J Pharmacol Exp Ther* **300**:97–104.
Cui JY, Gunewardena SS, Yoo B, Liu J, Renaud HJ, Lu H, Zhong XB, and Klaassen CD (2012) RNA-Seq reveals different mRNA abundance of transporters and their alternative transcript isoforms during liver development. *Toxicol Sci* **127**:592–608.
Cui YJ, Cheng X, Weaver YM, and Klaassen CD (2009) Tissue distribution, gender-divergent expression, ontogeny, and chemical induction of multidrug resistance transporter genes (Mdr1a, Mdr1b, Mdr2) in mice. *Drug Metab Dispos* **37**:203–210.
Duester G, Farrés J, Felder MR, Holmes RS, Höög JO, Parés X, Plapp BV, Yin SJ, and Jörnvall H (1999) Recommended nomenclature for the vertebrate alcohol dehydrogenase gene family. *Biochem Pharmacol* **58**:389–395.
Dunn RT, 2nd and Klaassen CD (1998) Tissue-specific expression of rat sulfotransferase messenger RNAs. *Drug Metab Dispos* **26**:598–604.
Fu ZD, Csanaky IL, and Klaassen CD (2012) Effects of aging on mRNA profiles for drug-metabolizing enzymes and transporters in livers of male and female mice. *Drug Metab Dispos* **40**:1216–1225.
Fu ZD and Klaassen CD (2014) Short-term calorie restriction feminizes the mRNA profiles of drug metabolizing enzymes and transporters in livers of mice. *Toxicol Appl Pharmacol* **274**:137–146.
Gonzalez FJ (2008) Regulation of hepatocyte nuclear factor 4 alpha-mediated transcription. *Drug Metab Pharmacokinet* **23**:2–7.
Janmohamed A, Hernandez D, Phillips IR, and Shephard EA (2004) Cell-, tissue-, sex- and developmental stage-specific expression of mouse flavin-containing monooxygenases (Fmos). *Biochem Pharmacol* **68**:73–83.
Jones RD, Taylor AM, Tong EY, and Repa JJ (2013) Carboxylesterases are uniquely expressed among tissues and regulated by nuclear hormone receptors in the mouse. *Drug Metab Dispos* **41**: 40–49.
Klaassen CD and Aleksunes LM (2010) Xenobiotic, bile acid, and cholesterol transporters: function and regulation. *Pharmacol Rev* **62**:1–96.
Klaassen CD and Lu H (2008) Xenobiotic transporters: ascribing function from gene knockout and mutation studies. *Toxicol Sci* **101**:186–196.
Klaassen CD and Slitt AL (2005) Regulation of hepatic transporters by xenobiotic receptors. *Curr Drug Metab* **6**:309–328.
Knight TR, Choudhuri S, and Klaassen CD (2007) Constitutive mRNA expression of various glutathione S-transferase isoforms in different tissues of mice. *Toxicol Sci* **100**:513–524.
Lee JM, Li J, Johnson DA, Stein TD, Kraft AD, Calkins MJ, Jakel RJ, and Johnson JA (2005) Nrf2, a multi-organ protector? *FASEB J* **19**:1061–1066.
Li J, Ning G, and Duncan SA (2000) Mammalian hepatocyte differentiation requires the transcription factor HNF-4alpha. *Genes Dev* **14**:464–474.
Li N, Hartley DP, Cherrington NJ, and Klaassen CD (2002) Tissue expression, ontogeny, and inducibility of rat organic anion transporting polypeptide 4. *J Pharmacol Exp Ther* **301**:551–560.
Lickteig AJ, Cheng X, Augustine LM, Klaassen CD, and Cherrington NJ (2008) Tissue distribution, ontogeny and induction of the transporters Multidrug and toxin extrusion (MATE) 1 and MATE2 mRNA expression levels in mice. *Life Sci* **83**:59–64.
Lu H, Chen C, and Klaassen C (2004) Tissue distribution of concentrative and equilibrative nucleoside transporters in male and female rats and mice. *Drug Metab Dispos* **32**:1455–1461.
Lu H, Gunewardena S, Cui JY, Yoo B, Zhong XB, and Klaassen CD (2013) RNA-sequencing quantification of hepatic ontogeny and tissue distribution of mRNAs of phase II enzymes in mice. *Drug Metab Dispos* **41**:844–857.
Lu H and Klaassen C (2006) Tissue distribution and thyroid hormone regulation of Pept1 and Pept2 mRNA in rodents. *Peptides* **27**:850–857.
Maher JM, Cherrington NJ, Slitt AL, and Klaassen CD (2006) Tissue distribution and induction of the rat multidrug resistance-associated proteins 5 and 6. *Life Sci* **78**:2219–2225.
Maher JM, Slitt AL, Cherrington NJ, Cheng X, and Klaassen CD (2005) Tissue distribution and hepatic and renal ontogeny of the multidrug resistance-associated protein (Mrp) family in mice. *Drug Metab Dispos* **33**:947–955.
Malone JH and Oliver B (2011) Microarrays, deep sequencing and the true measure of the transcriptome. *BMC Biol* **9**:34.
Nelson DR, Zeldin DC, Hoffman SM, Maltais LJ, Wain HM, and Nebert DW (2004) Comparison of cytochrome P450 (CYP) genes from the mouse and human genomes, including nomenclature recommendations for genes, pseudogenes and alternative-splice variants. *Pharmacogenetics* **14**: 1–18.
Parkinson A, Ogilvie BW, Buckley DB, Kazmi F, Czerwinski M, and Parkinson O (2013) Biotransformation of xenobiotics, in: Casarett & Doull's Toxicology: The Basic Science of Poisons (Klaassen CD ed), 185–367, McGraw-Hill, New York.
Peng L, Cui JY, Yoo B, Gunewardena SS, Lu H, Klaassen CD, and Zhong XB (2013) RNA-sequencing quantification of hepatic ontogeny of phase-I enzymes in mice. *Drug Metab Dispos* **41**:2175–2186.
Peng L, Yoo B, Gunewardena SS, Lu H, Klaassen CD, and Zhong XB (2012) RNA sequencing reveals dynamic changes of mRNA abundance of cytochromes P450 and their alternative transcripts during mouse liver development. *Drug Metab Dispos* **40**:1198–1209.
Petrick JS and Klaassen CD (2007) Importance of hepatic induction of constitutive androstane receptor and other transcription factors that regulate xenobiotic metabolism and transport. *Drug Metab Dispos* **35**:1806–1815.
Pratt-Hyatt M, Lickteig AJ, and Klaassen CD (2013) Tissue distribution, ontogeny, and chemical induction of aldo-keto reductases in mice. *Drug Metab Dispos* **41**:1480–1487.
Redinbo MR and Potter PM (2005) Mammalian carboxylesterases: from drug targets to protein therapeutics. *Drug Discov Today* **10**:313–325.
Renaud HJ, Cui JY, Khan M, and Klaassen CD (2011) Tissue distribution and gender-divergent expression of 78 cytochrome P450 mRNAs in mice. *Toxicol Sci* **124**:261–277.
Rosemond MJ and Walsh JS (2004) Human carbonyl reduction pathways and a strategy for their study in vitro. *Drug Metab Rev* **36**:335–361.
Selwyn FP, Cui JY, and Klaassen CD (2015) RNA-Seq Quantification of Hepatic Drug Processing Genes in Germ-Free Mice. *Drug Metab Dispos* **43**:1572–1580.
Shelby MK, Cherrington NJ, Vansell NR, and Klaassen CD (2003) Tissue mRNA expression of the rat UDP-glucuronosyltransferase gene family. *Drug Metab Dispos* **31**:326–333.
Slitt AL, Cherrington NJ, Hartley DP, Leazer TM, and Klaassen CD (2002) Tissue distribution and renal developmental changes in rat organic cation transporter mRNA levels. *Drug Metab Dispos* **30**:212–219.
Tanaka Y, Slitt AL, Leazer TM, Maher JM, and Klaassen CD (2005) Tissue distribution and hormonal regulation of the breast cancer resistance protein (Bcrp/Abcg2) in rats and mice. *Biochem Biophys Res Commun* **326**:181–187.
Thorrez L, Van Deun K, Tranchevent LC, Van Lommel L, Engelen K, Marchal K, Moreau Y, Van Mechelen I, and Schuit F (2008) Using ribosomal protein genes as reference: a tale of caution. *PLoS One* **3**:e1854.
Waxman DJ and Holloway MG (2009) Sex differences in the expression of hepatic drug metabolizing enzymes. *Mol Pharmacol* **76**:215–228.
Wood TC, Salavagionne OE, Mukherjee B, Wang L, Klumpp AF, Thomae BA, Eckloff BW, Schaid DJ, Wieben ED, and Weinshilboum RM (2006) Human arsenic methyltransferase (AS3MT) pharmacogenetics: gene resequencing and functional genomics studies. *J Biol Chem* **281**:7364–7373.
Yu L, Li-Hawkins J, Hammer RE, Berge KE, Horton JD, Cohen JC, and Hobbs HH (2002) Overexpression of ABCG5 and ABCG8 promotes biliary cholesterol secretion and reduces fractional absorption of dietary cholesterol. *J Clin Invest* **110**:671–680.
Zhang YK, Yeager RL, and Klaassen CD (2009) Circadian expression profiles of drug-processing genes and transcription factors in mouse liver. *Drug Metab Dispos* **37**:106–115.

**Address correspondence to:** Dr. Curtis D. Klaassen, Department of Environmental and Occupational Health Sciences, School of Public Health, University of Washington, 4225 Roosevelt Way NE, Suite #100, Box 354695, Seattle, WA 98105. E-mail: curtisklaassenphd@gmail.com